Volume 4, Issue 8— July — December - 2020

ECORFAN

Journal- Taiwan

ISSN-On line 2524-2121

ECORFAN®

ECORFAN-Taiwan

Chief Editor
VARGAS-DELGADO, Oscar. PhD

Executive Director
RAMOS-ESCAMILLA, María. PhD

Editorial Director
PERALTA-CASTRO, Enrique. MsC

Web Designer
ESCAMILLA-BOUCHAN, Imelda. PhD

Web Diagrammer
LUNA-SOTO, Vladimir. PhD

Editorial Assistant
SORIANO-VELASCO, Jesús. BsC

Translator
DÍAZ-OCAMPO, Javier. BsC

Philologist
RAMOS-ARANCIBIA, Alejandra. BsC

ECORFAN Journal-Taiwan, Volume 4, Issue 8, July-December 2020, is a journal edited semestral by ECORFAN. Taiwan, Taipei. YongHe district, Zhong Xin, Street 69. Postcode: 23445. WEB: www.ecorfan.org/taiwan/journal@ecorfan.org. Editor in Chief: VARGAS-DELGADO, Oscar. PhD. ISSN: 2524-2121. Responsible for the latest update of this number ECORFAN Computer Unit. ESCAMILLA-BOUCHÁN, Imelda. PhD, LUNA-SOTO, Vladimir. PhD, last updated December 31, 2020.

The opinions expressed by the authors do not necessarily reflect the views of the editor of the publication.

It is strictly forbidden to reproduce any part of the contents and images of the publication without permission of the National Institute for the Defense of Competition and Protection of Intellectual Property.

ECORFAN Journal- Taiwan

Definition of Journal

Scientific Objectives

Support the international scientific community in its written production Science, Technology and Innovation in the Field of Physical Sciences Mathematics and Earth sciences, in Subdisciplines of optical astronomy, optical characterization, optical encoder, experimental research, planetary magnetic fields, ultraviolet radiation, lasers, algorithms and optical waves.

ECORFAN-Mexico SC is a Scientific and Technological Company in contribution to the Human Resource training focused on the continuity in the critical analysis of International Research and is attached to CONACYT-RENIECYT number 1702902, its commitment is to disseminate research and contributions of the International Scientific Community, academic institutions, agencies and entities of the public and private sectors and contribute to the linking of researchers who carry out scientific activities, technological developments and training of specialized human resources with governments, companies and social organizations.

Encourage the interlocution of the International Scientific Community with other Study Centers in Mexico and abroad and promote a wide incorporation of academics, specialists and researchers to the publication in Science Structures of Autonomous Universities - State Public Universities - Federal IES - Polytechnic Universities - Technological Universities - Federal Technological Institutes - Normal Schools - Decentralized Technological Institutes - Intercultural Universities - S & T Councils - CONACYT Research Centers.

Scope, Coverage and Audience

ECORFAN Journal- Taiwan is a Journal edited by ECORFAN-Mexico S.C in its Holding with repository in Taiwan, is a scientific publication arbitrated and indexed with semester periods. It supports a wide range of contents that are evaluated by academic peers by the Double-Blind method, around subjects related to the theory and practice of optical astronomy, optical characterization, optical encoder, experimental research, planetary magnetic fields, ultraviolet radiation, lasers, algorithms and optical waves with diverse approaches and perspectives , That contribute to the diffusion of the development of Science Technology and Innovation that allow the arguments related to the decision making and influence in the formulation of international policies in the Field of Physical Sciences Mathematics and Earth sciences. The editorial horizon of ECORFAN-Mexico® extends beyond the academy and integrates other segments of research and analysis outside the scope, as long as they meet the requirements of rigorous argumentative and scientific, as well as addressing issues of general and current interest of the International Scientific Society.

Editorial Board

VERDEGAY - GALDEANO, José Luis. PhD
Universidades de Wroclaw

GONZALEZ - ASTUDILLO, María Teresa. PhD
Universidad de Salamanca

MAY - ARRIOJA, Daniel. PhD
University of Central Florida

RODRÍGUEZ-VÁSQUEZ, Flor Monserrat. PhD
Universidad de Salamanca

VARGAS - RODRIGUEZ, Everardo. PhD
University of Southampton

GARCÍA - RAMÍREZ, Mario Alberto. PhD
University of Southampton

TORRES - CISNEROS, Miguel. PhD
University of Florida

RAJA - KAMARULZAMAN, Raja Ibrahim. PhD
University of Manchester

ESCALANTE - ZARATE, Luis. PhD
Universidad de Valencia

Arbitration Committee

JIMENEZ - CONTRERAS, Edith Adriana. PhD
Instituto Politécnico Nacional

BELTRÁN - PÉREZ, Georgina. PhD
Instituto Nacional de Astrofísica Óptica y Electrónica

ANZUETO - SÁNCHEZ, Gilberto. PhD
Centro de Investigaciones en Óptica

GUZMÁN - CHÁVEZ, Ana Dinora. PhD
Universidad de Guanajuato

CANO - LARA, Miroslava. PhD
Universidad de Guanajuato

OROZCO - GUILLÉN, Eber Enrique. PhD
Instituto Nacional de Astrofísica Óptica y Electrónica

ROJAS - LAGUNA, Roberto. PhD
Universidad de Guanajuato

JAUREGUI - VAZQUEZ, Daniel. PhD
Universidad de Guanajuato

GARCÍA - GUERRERO, Enrique Efrén. PhD
Centro de Investigación Científica y de Educación Superior de Ensenada

GUERRERO-VIRAMONTES, J Ascención. PhD
Universidad de Guanajuato

IBARRA-MANZANO, Oscar Gerardo. PhD
Instituto Nacional de Astrofísica, Óptica y Electrónica

Assignment of Rights

The sending of an Article to ECORFAN Journal- Taiwan emanates the commitment of the author not to submit it simultaneously to the consideration of other series publications for it must complement the Originality Format for its Article.

The authors sign the Authorization Format for their Article to be disseminated by means that ECORFAN-Mexico, S.C. In its Holding Taiwan considers pertinent for disclosure and diffusion of its Article its Rights of Work.

Declaration of Authorship

Indicate the Name of Author and Coauthors at most in the participation of the Article and indicate in extensive the Institutional Affiliation indicating the Department.

Identify the Name of Author and Coauthors at most with the CVU Scholarship Number-PNPC or SNI-CONACYT- Indicating the Researcher Level and their Google Scholar Profile to verify their Citation Level and H index.

Identify the Name of Author and Coauthors at most in the Science and Technology Profiles widely accepted by the International Scientific Community ORC ID - Researcher ID Thomson - arXiv Author ID - PubMed Author ID - Open ID respectively.

Indicate the contact for correspondence to the Author (Mail and Telephone) and indicate the Researcher who contributes as the first Author of the Article.

Plagiarism Detection

All Articles will be tested by plagiarism software PLAGSCAN if a plagiarism level is detected Positive will not be sent to arbitration and will be rescinded of the reception of the Article notifying the Authors responsible, claiming that academic plagiarism is criminalized in the Penal Code.

Arbitration Process

All Articles will be evaluated by academic peers by the Double Blind method, the Arbitration Approval is a requirement for the Editorial Board to make a final decision that will be final in all cases. MARVID® is a derivative brand of ECORFAN® specialized in providing the expert evaluators all of them with Doctorate degree and distinction of International Researchers in the respective Councils of Science and Technology the counterpart of CONACYT for the chapters of America-Europe-Asia- Africa and Oceania. The identification of the authorship should only appear on a first removable page, in order to ensure that the Arbitration process is anonymous and covers the following stages: Identification of the Journal with its author occupation rate - Identification of Authors and Coauthors - Detection of plagiarism PLAGSCAN - Review of Formats of Authorization and Originality-Allocation to the Editorial Board-Allocation of the pair of Expert Arbitrators-Notification of Arbitration -Declaration of observations to the Author-Verification of Article Modified for Editing-Publication.

Instructions for Scientific, Technological and Innovation Publication

Knowledge Area

The works must be unpublished and refer to topics of optical astronomy, optical characterization, optical encoder, experimental research, planetary magnetic fields, ultraviolet radiation, lasers, algorithms and optical waves and other topics related to Physical Sciences Mathematics and Earth sciences.

Presentation of the content

In the first article we present, *Optimizing the removal of fluorescence and shot noise in Raman Spectra of minerals by ANFIS and moving averages filter*, by CABRERA-CABAÑAS, Reinier, LUNA-ROSAS, Francisco Javier, MARTINEZ-ROMO, Julio César and HERNÁNDEZ-VARGAS, Marco Antonio, with adscription in the Instituto Tecnológico de Aguascalientes, in the next article we present, *Artificial vision system for the prevention of injuries in the upper back and neck areas based on the OpenPose algorithm*, by GARCÍA-CERVANTES, Heraclio, CARDONA-VILLALPANDO, Juan Carlos, BLANCO-MIRANDA, Alan David and CARRILLO-HERNÁNDEZ, Didia, with adscription in the Universidad Tecnológica de León, in the next article we present, *Characterization of a copper susceptor sensitive to solar IR and UV radiation*, by ZARATE-CORONA, José, TELOXA-REYES, Julio and AGUILAR-GALVAN, Daniel, in the last article we present, *Comparative study of thermal efficiency of flat spiral vs. conical spiral in a parabolic solar collector*, by AVALOS-SANCHEZ, Tomás, ROBLES-VELAZQUEZ, Patricia and PRADO-SALAZAR, María.

Content

Article **ECORFAN Journal- Taiwan**
December, 2020 Vol.4 No.8 1-12

Optimizing the removal of fluorescence and shot noise in Raman Spectra of minerals by ANFIS and moving averages filter

Optimización del proceso de eliminación de la fluorescencia y el ruido de disparo en espectros Raman de minerales mediante ANFIS y el filtro de medias móviles

CABRERA-CABAÑAS, Reinier†*, LUNA-ROSAS, Francisco Javier, MARTINEZ-ROMO, Julio César and HERNÁNDEZ-VARGAS, Marco Antonio

Instituto Tecnológico de Aguascalientes, Computing Science Department, Av. A. López Mateos 1801 Ote. Col. Bona Gens, C.P. 20256, Aguascalientes, Ags., México

ID 1st Author: *Reinier, Cabrera-Cabañas* / **CVU CONACYT ID**: 765973

ID 1st Coauthor: *Francisco Javier, Luna-Rosas* / **ORC ID**: 0000-0001-6821-4046, **arXiv Author ID**: arXivFco19, **CVU CONACYT ID**: 87098

ID 2nd Coauthor: *Julio César, Martinez-Romo* / **ORC ID**: 0000-0001-6242-5248

ID 3rd Coauthor: *Marco Antonio, Hernández-Vargas* / **ORC ID**: 0000-0002-8146-9307

DOI: 10.35429/EJT.2020.8.4.1.12 Received October 02, 2020; Accepted November 29, 2020

Abstract

Raman spectroscopy is a non-destructive and non-contact technique that requires minimal sample preparation so it can be used to identify a wide range of minerals and gemstones. This optical technique is capable of measuring vibrational modes of biomolecules, allowing their identification from the correct location of the Raman bands, one of the main challenges is the elimination of spectral noise composed of (a) fluorescence background and (b) high frequency noise. The objective of the article was to demonstrate that using ANFIS (Neuro Fuzzy Adaptive Inference System) in combination with moving averages filter on the MATLAB multicore platform we can eliminate these disturbances and optimize response time in the preprocessing of large volumes of data while maintaining the spectral meaning related to the structure and/or composition of the mineral to be validated.

Spectroscopy, Fluorescence, Optimum Design

Resumen

La espectroscopía Raman es una técnica no destructiva y de no contacto que requiere una preparación mínima de la muestra por lo que puede usarse para identificar una amplia gama de minerales y piedras preciosas. Esta técnica óptica es capaz de medir los modos vibratorios de las moléculas, permitiendo su identificación desde la correcta ubicación de las bandas Raman, uno de los principales desafíos es la eliminación del ruido espectral compuesto por (a) fondo de fluorescencia y (b) ruido de alta frecuencia. El objetivo del artículo fue demostrar que utilizando ANFIS (Sistema Adaptativo de Inferencia Neuro-difusa) en combinación con el filtro de medias móviles en la plataforma multinúcleo MATLAB podemos eliminar estas alteraciones y optimizar el tiempo de respuesta en el preprocesamiento de grandes volúmenes de datos manteniendo el significado espectral clave relacionado con la estructura y/o composición del mineral a validar.

Espectroscopía, Fluorescencia, Diseño óptimo

Citation: CABRERA-CABAÑAS, Reinier, LUNA-ROSAS, Francisco Javier, MARTINEZ-ROMO, Julio César and HERNÁNDEZ-VARGAS, Marco Antonio. Optimizing the removal of fluorescence and shot noise in Raman Spectra of minerals by ANFIS and moving averages filter. ECORFAN Journal-Taiwan. 2020. 4-8: 1-12

* Author correspondence (cabrera1988reinier@gmail.com)
† Researcher contributing as first author.

© ECORFAN Journal-Taiwan

1. Introduction

Raman spectroscopy is one of the most used techniques in mining for the analysis and identification of compound. The geological characterization for example provides information about the formation of a site and its history. This process requires detailed morphological, physical, and compositional analyzes of rocks and sediments (Ishikawa & Gulick, 2013). Raman method is a high-resolution photonic technique that provides in a few seconds chemical and structural information of almost any organic and / or inorganic material or compound, allowing its identification.

The study by Raman spectroscopy is based on the analysis of the light scattered by a material by making a monochromatic light beam strike it, when this happens a small portion of the light is inelastically scattered, undergoing slight changes in frequency that are characteristic of the material analyzed and independent of the frequency of the incident light. This technique is currently being applied in multiple scientific areas, such as Physics and Chemistry, Biochemistry, virus detection (Yeh et al., 2020). However, one of the great problems of Raman spectra is that the Raman scattering (RS), which characterizes the composition of the sample, is accompanied by noise generated by the measuring instrument, external sources, and noise due to fluorescence. The latter may be orders of magnitude greater than the Raman signal, preventing obtaining information associated with its molecular composition. Therefore, it is necessary to eliminate the noise in the spectra before the analysis stage.

Noise removal is one of the most important data processing operations. Despite its wide use in various types of signals, there is no general strategy to carry out this procedure, since it largely depends on the problem treated, the signal-to-noise ratio (S / N) and the shape of the signals. Noise elimination process must be carried out with special care to avoid loss of information, and to adapt to the signal to be analyzed. To noise elimination, two different approaches have been used: the experimental and the computational. The methods that use the experimental approach are based on adjustments or improvements to the instrumentation and these include shifted excitation and time-limited systems (Gebrekidan et al., 2016).

Experimental methods like the previous ones are a little complex because they involve long acquisition times, for these reasons the use of computational methods has increased due to their speed, easy implementation, and low cost. Some computational methods that stand out include adjustment methods, highlighting the modified multipolinomial adjustment method and the Vancouver Algorithm (Lieber & Ahadevan-jansen, 2003; Zhao, Lui, Mclean, & Zeng, 2007), the methods based on wavelet transforms (Gebrekidan, Knipfer, & Braeuer, 2020) and the morphological algorithms (Javier et al., 2018).

In this work, ANFIS (Adaptive Neuro-Fuzzy Inference System), an integrating system between neural networks and fuzzy-logic that has previously been applied as an artificial intelligence tool in some areas such as Architecture, in the automotive industry, in Biochemistry and in Medicine (Übeyli, 2008) is used to characterize the contribution of fluorescence noise that is generated in Raman signals from different minerals, the procedure consists of developing an algorithm that allows to subtract the Raman peaks from the signal until a continuous signal at intervals is obtained, that signal will act as input to the diffuse neural network; the same, through an own adjustment system using the backpropagation error will adjust the background curve of the signal and filling in the empty spaces where the peaks were. This obtained signal will be assumed as the fluorescence background masking the signal and will be subtracted from the original signal. To eliminate small fluctuations that occur around the average value of the signal, moving averages filters are used which allow smoothing the signal, suppressing high-frequency noise.

This procedure ensures that the signal is clean of noise and, in a position to be correctly identified for future diagnostic and prediction procedures. Furthermore, in this article we demonstrate that it is possible to optimize the response time in the pre-processing of Raman signals of minerals, when we eliminate fluorescence and shot noise in large quantities of data, achieving an improvement of 53.60% in relation to the processing of data sequentially, which makes it a valuable tool in the field of mining for future applications of diagnosis and quick recognition of minerals but this can be used in other areas like medicine to quick prediction of diseases.

ISSN 2524-2121
ECORFAN® All rights reserved

CABRERA-CABAÑAS, Reinier, LUNA-ROSAS, Francisco Javier, MARTINEZ-ROMO, Julio César and HERNÁNDEZ-VARGAS, Marco Antonio. Optimizing the removal of fluorescence and shot noise in Raman Spectra of minerals by ANFIS and moving averages filter. ECORFAN Journal-Taiwan. 2020

2. Materials and methods

2.1 (Adaptative Neuro-Fuzzy Inference System)

ANFIS (Adaptive Neuro Fuzzy Inference System) integrates Neural Networks with fuzzy logic inheriting the characteristics of both, allows you to tune or create the rule base of a fuzzy system using the backpropagation algorithm from the data collection of a process. It is an architecture functionally equivalent to a fuzzy rule system based on Takagi and Sugeno mode (Sugeno & Kang, 1988; Takagi & Sugeno, 1984).

The Neuro-Diffuse system is a traditional diffuse system in which each stage can be represented by a layer of neurons to which neural network learning capabilities can be provided to optimize the knowledge of the system. By having trainable parameters, the delta rule algorithms and backpropagation error are applicable (Jang, Sun, & Mizutani, 1997). Some parameters allow to establish the training set of the ANFIS system, and some common rules presented by the first order fuzzy model are necessary.

2.2 Moving averages

Moving Averages is a fairly simple prediction method that has been used in commerce and has not been altered for more than half a century (Soberón-celedón, Molina-contreras, Frausto-reyes, & Carlos, 2016). A window of size N is selected, and the mean or average of the variable for the N data is obtained, allowing the average to move as the new data of the variable in question are observed. This smoothes out possible strong oscillations or outliers.

The increase of any moving average depends exclusively on the shape of the function f and the size of the selected window. The mean movement of order N (MA_f) of a series f of values $Y1, Y2, Y3, \dots Yn$ is defined by the sequence of values corresponding to the arithmetic means:

$$MA_f = \left(\frac{Y_1+Y_2+Y_N}{N}; \frac{Y_2+Y_3+Y_{N+1}}{N}; \frac{Y_3+Y_4+Y_{N+2}}{N}; \dots\right) \quad (1)$$

Where $Y_1, Y_2, Y_3, \dots, Y_N$ are the most recent observations of the closed interval; N is the size of the Interval within the function f.

2.3 Parallel Computing

Parallel computing is a form of computation in which many instructions are performed simultaneously, operating over the principle that big problems can often be divided into smaller ones, which are then solved simultaneously (in parallel).

The hardware that supports parallel computing consists of multicore computers, symmetric multiprocessors, distributed computers such as task clusters stations, and specialized parallel processors such as FPGA, GPU, and built in circuits of specific applications (AISC). With the development of hardware that supports parallel programming, especially the development of multicore computers, parallel programming architectures become more important than before (Gao, Kemao, Wang, Lin, & Seah, 2009).

The most common forms of parallelism, include: task parallelism, pipeline parallelism, and data parallelism (Gao et al., 2009). In the task parallelism, also known as functional parallelism, is a development structure in which, independent figures from parts of a method can be performed simultaneously in different processors. In the case of pipeline parallelism, the problem is separated in a series of tasks. Any of the tasks will be performed in a separate process or processor. Each parallel process is usually referred to as a pipeline state.

The exit as a pipeline state serves as the entrance of another state, therefore, in a given time each pipeline state is working over a different dataset. The data parallelism is mainly centered over the same process that will be applied simultaneously over different parts of a dataset. Let us say, similar operating sequences or functions are carried out in parallel over a large element data structure.

Moreover, if given enough parallel resources, the computing time of the data structure in parallel is usually independent from the problem size. One of the parallelism methods mentioned previously or their combination should be used in parallel applications.

ISSN 2524-2121
ECORFAN® All rights reserved

3. Experiments

Raw Raman spectra were obtained from a complete set of high-quality spectral data from well characterized minerals shared in the project RRUFF. The database was prepared by collaborators from universities from different parts of the world and shared with the science. Several Raman spectrometers are used for to get RRUFF Raman samples but in this work were selected samples taken with a commercial Thermo Almega XR with 532 nm laser. 10500mineral samples were collected from different sources and universities around the world.

4. Results and Discussion

4.1 Description of the proposed algorithm for fluorescence and shot noise reduction

As previously mentioned, the Raman signal is made up of the useful signal, (characteristic of the molecular vibrations that occur inside the excited molecule) and a noise signal inherent in the measurement process, mainly high-frequency noise, and fluorescence background.

$$Y = X_{true} + b + n \quad (2)$$

Where X_{true} is the Raman spectra free of noise and fluorescence, b is the background fluorescence, n is the noise in the signal and finally Y is the raw Raman signal acquired with the spectrometer containing fluorescence and shot noise. In such a way that to obtain a noise-free signal it is necessary to subtract the identified background fluorescence and shot noise from the raw signal.

The strategy followed is to design a mechanism to eliminate possible peaks in the raw Raman signal by detecting their start and end points. By suppressing these peaks, we will have a continuous signal at intervals such as the one shown in Figure 5, the objective of using ANFIS is to apply an interpolation to determine the possible shape of the fluorescence signal in the empty spaces of the signal, to finally subtract it from the measured spectrum. Figure1 shows a diagram highlighting each of the stages involved in the fluorescence removal process.

Stage 1. Load the Raman signal. In this step, the data vector is loaded from an Excel file, it contains two columns corresponding to the intensity values of the spectrum and the shift Raman respectively. In Figure 2 we have an example of a raw Raman spectrum corresponding to calcite.

Stage 2. Normalizing the data. This stage was performed in order to keep the signal under the same scale on the two coordinate axes, it was achieved through an interpolation algorithm, on the y-axis the maximum and minimum values of the spectrum were calculated, the minimum value is subtracted of the original spectrum and the result is divided by the maximum value, leaving the intensity values between 0 and 1, on the x-axis an arbitrary value of 574 values corresponding to the length of the data was taken. This is the best way to work with the signals because the signals would be on the same scale and the slope on each Raman signal will be easily located and very similar.

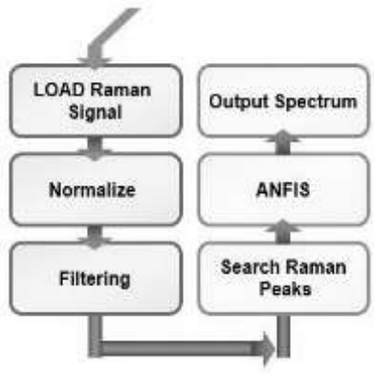

Figure 1 Program sequence designed to eliminate noise in Raman spectra

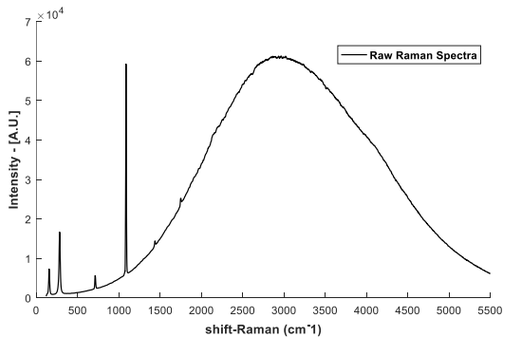

Figure 2 Raman signal of calcite ($CaCO_3$) without processing

ECORFAN® All rights reserved

Stage 3. Signal Filtering. A moving averages filter is applied with the purpose of smoothing the signal as a previous step to the correction of the baseline, the procedure is performed with a vector of fixed size previously defined and the central part of the result that is equal in size is rescued to the original data. With this method it is possible to overshadow the high frequency noise that affects the spectrum and dissolve the small peaks in the signal that can cause confusion in the interpretation of the data. Figure 3 shows the high frequency noise that was subtracted from the calcite Raman signal in the range of 1600 to 2400 cm^{-1}.

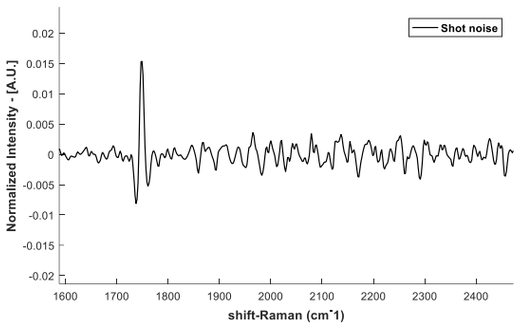

Figure 3 Shot noise removed from the Raman signal of calcite by moving averages Filter in the range of 1600 to 2400 cm^{-1}

Stage 4. Looking for Raman peaks candidates. With this objective, different algorithms were implemented that allow detecting all the signal peaks and subtracting them from the original signal, considering their starting and ending points.

The way this problem is solved is as follows:

1- Initially all the maximum points of the signal are discovered, for this it was necessary to implement a window algorithm with a window size equal to 15 samples, when we sampling the signal in this way the maximum values inside the window were found and assumed as possible Raman peaks if they were centered in the window; if they bow to one side they are discarded.

Through this method, we detect the portions of the spectrum that may have a peak shape and that could later be identified as legitimate Raman peaks.

2- Once all the possible signal peaks are obtained, the maximum values are taken for evaluation, keeping the same window size is evaluated point by point from the maximum value descending on both sides of the possible peak (to the right is increased by 1 unit and the left is decreased by one unit with respect to the x-axis), a least squares procedure is applied at each point to obtain the equation of the line that best describes the points corresponding to each window, the angle of inclination is calculated in each step respect to the abscissa and is compared taking as a criterion that the inclination of the peak is represented by an angle of more than 60º since for smaller angles they would make the appearance of the peak disappear and the structure of the signal would be affected with the introduction of morphological errors. The point where the condition is not met is taken as the starting and ending point of the peak.

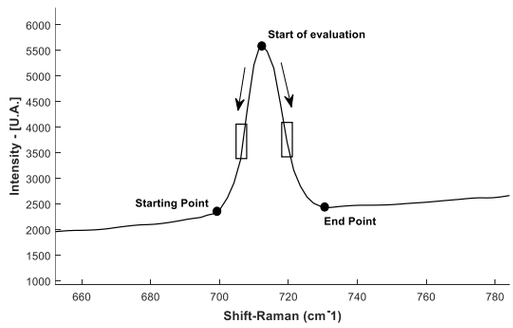

Figure 4 Evaluation to find the start and end points of the peak

In Figure 4 we can observe the procedure described above. We can see that the start and end points of the peak (points where the condition is not met) do not have the same height, and the rectangles try to represent the angle that is formed between the points with respect to the axis of the abscissa.

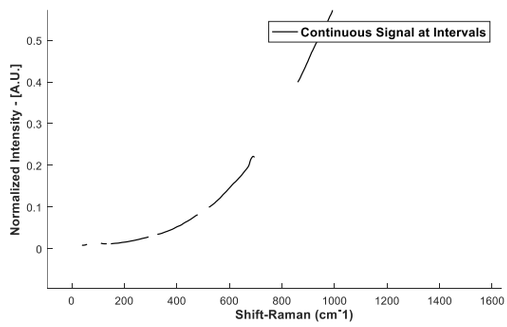

Figure 5 Raman signal continues at intervals with the peak regions removed

ECORFAN® All rights reserved

Stage 5. ANFIS, configuration developed. ANFIS is used at the junction of the points where each peak detected in the previous stage begins and ends. An adaptive network is constructed functionally equivalent to the fuzzy model Sugeno type whose scheme can be seen in Figure 6.

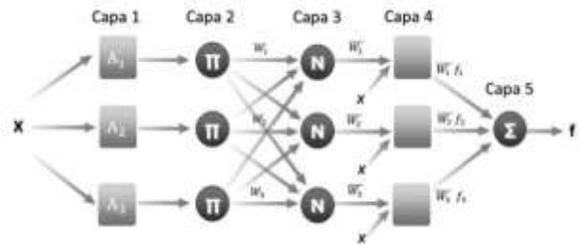

Figure 6 ANFIS network structure. One input, three rules one output

The procedure to apply ANFIS Will be explained step by step:

Preparation of the data. For explanatory purposes the vector containing the signal will be known as y or output and the vector containing the abscissa data will be known as x or input. Those definitions allow us to define the training set of the ANFIS system.

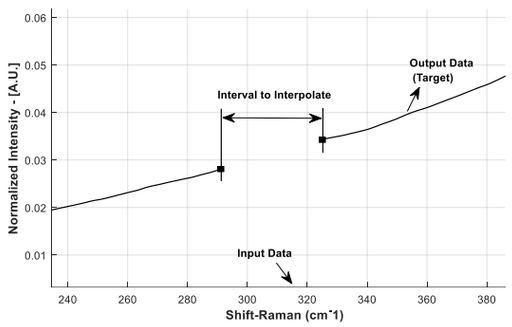

Figure 7 Portion of the spectrum selected for training

Training with ANFIS. To explain the training procedure a portion of the spectrum has been selected, the values required for training are the scale in which the Raman peaks do not appear on the x-axis as input and the amplitude y as the output variable or target that presents the Raman peak. In Figure 7 we can see a portion of the spectrum that we selected for illustrative purposes where the representation of the training vectors is framed on the x and y-axes. The scale we take on the x-axis goes from 941.7 cm^{-1} to 1051 cm^{-1} as the input variable and the amplitude y as the output or target variable.

In the mentioned interval there is a Raman peak in the interval between 962.4 cm^{-1} and 1032 cm^{-1}.

Forward propagation phase: Layer 1 (see Figure 6) receives vector X and calculates the degree of membership $\mu_{Ak}(X)$ of the fuzzy set for each of the values X_i of the vector according to the membership function A_k associated with each input; in this case a gaussian membership function with three trainable parameters

$$A_k = \text{gauss}\,(\text{x}, \sigma, \text{c}) = e^{-\left(\frac{x-c}{\sigma}\right)^2} \quad (3)$$

In layer 2 (layer π) the output of the nodes is the product of all the input signals, but in this case the antecedent is formed by a unique condition (if x is ...), therefore the output of this layer $w = \mu_{Ak}(X)$

In layer 3 (layer N) every element $w_{i,j}$ is normalized to the sum $w_{i,1}+w_{i,2}+w_{i,3}$

$$\overline{w_i} = \frac{w_i}{w_1+w_2} \quad , i = 1, 2 \quad (4)$$

In the next stage of forward propagation layers 4 and 5 of the presented network structure are involved. The parameters (consequent parameters) p, q and r of the linear models that are weighted by the inputs are candidates for training in this phase and represent the inferred fuzzy output set. Every node in this layer is an adaptive node with a function:

$$\overline{w}_i f_i = \overline{w}_i(p_i(x) + q_i(y) + r_i) \quad (5)$$

In which f_i are those described in the rules of the fuzzy system (Sugeno & Kang, 1988). Finally, the defuzzification is carried out, the outputs are processed and integrated as a summation of all the input signals.

$$output = \sum \overline{w}_i f_i \quad (6)$$

The backpropagation algorithm uses the sum of the square error between the desired output and the output of the ANFIS system to adjust all the trainable parameters of layer 1 of the system. The error is back propagated from layer m to layer m-1; thus, from layer 5 to 4 there is an error signal of 5-4, from 4 to 3 the signal is 4-3, and so on, until the error signal 2-1 is reached.

ISSN 2524-2121
ECORFAN® All rights reserved

The latter is the one used to adjust the nonlinear trainable elements of layer 1, which are the parameters σ and c of the fuzzy sets A_k. The described process of forward propagation and back propagation is performed iteratively up to a certain number of epochs (100 in this case) or until the error decreases to a specific value.

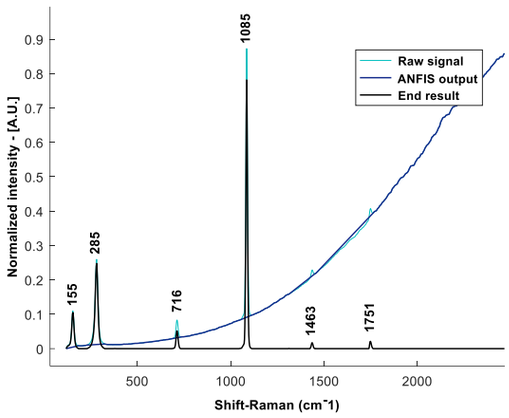

Figure 8 Raman spectrum corresponding to Calcite ($CaCO_3$). In cyan the Raman spectrum after the application of the moving averages filtering, in blue the fluorescence background rescued by the final adjustment of ANFIS and in black the noise-free Raman spectrum

Figure 8 shows the final result in three graphs; we can see the result of applying moving averages filtering and the ANFIS algorithm to eliminate the fluorescence and the shot noise signals and get a spectrum that allows us to make a prediction with the minimum error rate, the first one, of cyan color, shows the values of the Raman spectrum of $CaCO_3$ after the application of moving average filters, the blue one, shows the output values of ANFIS that translates as the fluorescence background of the analyzed spectrum and Finally, in black, the noise-free Raman spectrum after applying the subtraction of the spectra mentioned above. Raman spectra of the carbonates studied are well-known at ambient conditions.

The optical vibrations can be separated into internal vibrations of the CO_3 group (lying between 700 and 1500 cm^{-1}) and external or lattice vibrations involving translation and liberations of the CO_3 groups relative to the Ca atom (100-500 cm^{-1}). The vibrations of the "free" CO_3 group (vl: symmetric stretch; v3 asymmetric stretch; v2: out-of-plane bend; v4 in-plane bend) have been observed and assigned in Raman spectra of the carbonates of both rhombohedral and orthorhombic symmetry.

The site symmetry of the CO_3 group is determined by the cation environment and modifies the selection rules (i.e. the number of bands observed), and the frequencies to a small extent, when compared with the free group. In this figure we can observe the vibrational modes located in the low frequency range at 155, y 285 cm^{-1} that represent external or lattice modes, resulting from the interactions between Ca^{2+} and CO_3^{2-} ions. The high frequency vibrational modes at 716, 1085 and 1463 cm^{-1} represent internal modes of the CO_3^{2-} group(Gillet, Biellmann, Reynard, & McMillan, 1993).

4.2 Method Check

In this section, the efficiency of the method used to suppress noise in Raman spectra through ANFIS and moving averages filter will be verified. The raw spectra of some minerals such as Cerussite, Calomel, Hematite and Zircon will be used for this purpose. The spectra of these raw minerals are exposed, and the method described above is applied to each of them, obtaining similar results to those of the consulted literature. Each of the spectra with the most significant occurrences detected after denoising are detailed below.

Cerussite ($PbCO_3$)

The common simple pock-forming carbonates can be divided in three main groups: (1) the calcite group, (2) the dolomite group, and (3) the aragonite group. The cerussite ($PbCO_3$) is member of the aragonite group, is metastable under atmospheric conditions and therefore is less commonly found in nature than calcite. Aragonite is found in the calcareous skeletons of many organisms (e.g., shells of mollusks).

The molecular vibrations can be separated in (v_1: symmetric stretch; v_3: asymmetric stretch; v_2: out-of-plane bend; v_4: in-plane bend) have been observed and assigned in Raman spectra, v_1 at 1054 cm^{-1} is the most obvious feature in this region. The FWHM of this band is much narrower that other combination bands.

ISSN 2524-2121
ECORFAN® All rights reserved

This and the fact that there is a nearly constant shift between the satellite band and the main v1 band in all aragonites suggest that combination bands are an unlikely explanation, in Figure 9 we can see v_2 at 837 cm^{-1} corresponding with the partial covalent bond between the lead on the covalent ions, v_3 at 1376 and 1476 cm^{-1} are attributed to the carbonate bending mode of cerussite, v_4 at 681cm-1 is attributed to the bending mode of the carbonate ion. The lattice vibrations band of cerussite are detected at 132 and 243 cm-1 corresponding to the lower frequencies(Martens, Rintoul, Kloprogge, & Frost, 2004).

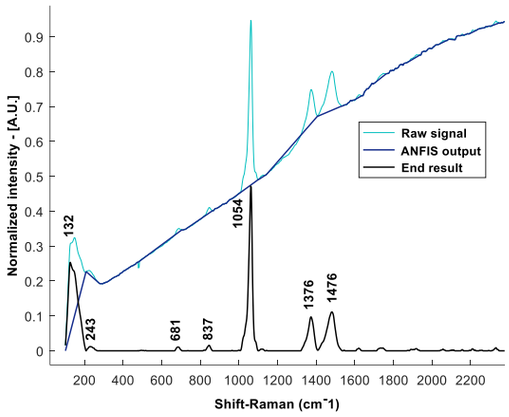

Figure 9 Raman spectrum corresponding to Cerussite (PbCO3). In cyan the Raman spectrum after the application of the moving averages filtering, in blue the fluorescence background rescued by the final adjustment of ANFIS and in black the noise-free Raman spectrum

Zircon ($ZrSiO_4$)

Zircon ($ZrSiO_4$) is an unusually common and widely distributed mineral, but the crystals are rare. The structure of zircon contains Si in tetrahedral coordination by oxygen, and Zr in 8-fold coordination by oxygen in the form of triangular-faced dodecahedra, these structural features indicate that there is a strong repulsive interaction between the neighboring Zr and Si atoms. In Figure 10 we can see the Raman spectrum of the Zircon after ANFIS and moving averages filter, the wavenumbers of all the phonon modes in zircon are shown 130 cm^{-1} represent a rigid rotation of the SiO4 , the 223 cm^{-1} is a rigid rotation of the SiO_4 around the a-axis, shearing of the Zr, 341cm^{-1} is a rigid rotation of the SiO_4 around the a-axis, shearing of the Zr, in 437cm^{-1} there are a Symmetric flattening of the SiO_4 along the c-axis, and in 1008 cm-1 have a stretching Si of Si–O that is anti-symmetric with respect to the O_{sh}–O_{sh} edge of SiO_4 .

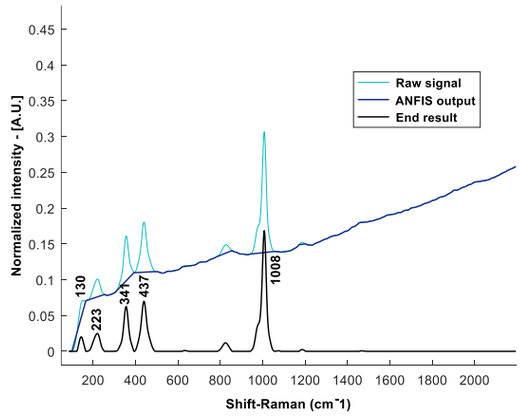

Figure 10 Raman spectrum corresponding to Zircon (ZrSiO4). In cyan the Raman spectrum after the application of the moving averages filtering, in blue the fluorescence background rescued by the final adjustment of ANFIS and in black the noise-free Raman spectrum

Calomel (Hg_2Cl_2)

Calomel is a mercury (I) chloride mineral with formula Hg_2Cl_2, mainly used nowadays as a component of reference electrodes in electrochemistry, this compound was a widespread and popular medicine until it fell out of use at the endo of 19th century due to its toxicity, and a material caller mercury white is referred to in 16th century technical literature on painting. The spectrum showed in Figure 11 Reveal two lines whose polarization correspond to fully symmetric vibrations at 167 and 275 cm^{-1}, matching those of a reference spectrum of calomel (Crippa, Legnaioli, Kimbriel, & Ricciardi, 2020).

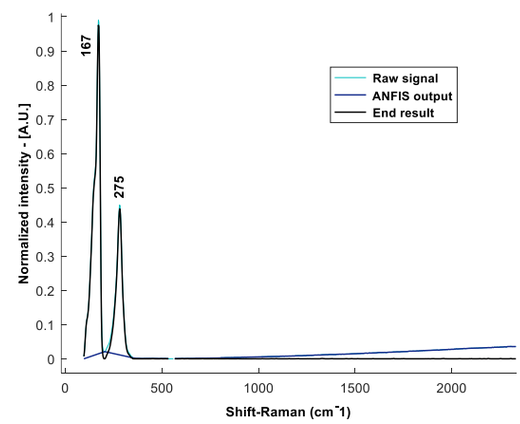

Figure 11 Raman spectrum corresponding to Calomel (Hg2Cl2). In cyan the Raman spectrum after the application of the moving averages filtering, in blue the fluorescence background rescued by the final adjustment of ANFIS and in black the noise-free Raman spectrum

ISSN 2524-2121
ECORFAN® All rights reserved

Hematite (Fe_2O_3)

The hematite (Fe_2O_3) is a mineral in felsic igneous rocks, a late-stage sublimate in volcanic rocks, and in high-temperature hydrothermal veins. A product of contact metamorphism and in metamorphosed banded iron formations. A common cement in sedimentary rocks and a major constituent in oolitic iron formations. Abundant on weathered iron-bearing minerals.
In the Raman spectrum of the hematite showed in Figure 12 are expected seven phonon lines, namely two A_{1g} modes (225 and 498 cm^{-1}) and five E_g modes (246, 299, 410, 497 and 613 cm^{-1}) Hematite is an antiferromagnetic material and the collective spin movement can be excited in what is called a magnon. The intense feature at 1320 cm^{-1} is assigned to a two-magnon scattering which arises from the interaction of two magnons created on antiparallel close spin sites(De Faria, Venâncio Silva, & De Oliveira, 1997).

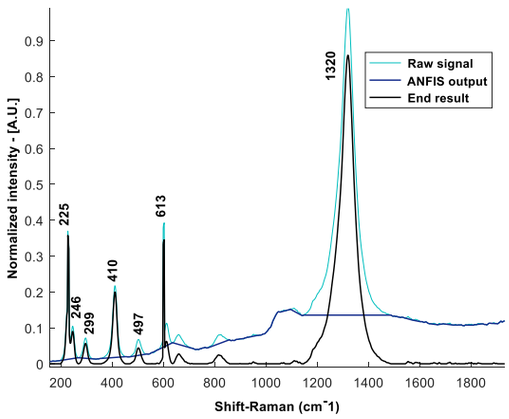

Figure 12 Raman spectrum corresponding to Hematite (Fe2O3). In cyan the Raman spectrum after the application of the moving averages filtering, in blue the fluorescence background rescued by the final adjustment of ANFIS and in black the noise-free Raman spectrum

4.3 Optimum design in the removal of fluorescence and shot noises in Raman spectrum of minerals

Today, data is in all kinds of formats; from traditional databases to hierarchical data stores created by end users, through OLAP systems, text documents, email, measurement data, signal data, video, audio, stock information and financial transactions, among many others. According to some calculations, 80% of the data of the organizations are not numerical (Prajapati, 2013). However, these should also be included in the analysis and decision-making process.

Speed designates how quickly data is generated and how fast it must be processed to satisfy demand. In this section we show how we can optimally preprocess high-volume of Raman signals from mineral examples (data parallelism) by applying MATLAB multicore technology (Cartagena, Juan, Rodríguez, & Autor, 2010). As we have seen, there are many sources of noise that attack the weak Raman signal. In order to achieve material identification, it is essential to have a good signal-to-noise ratio in the Raman spectrum.

Currently, there are different methods implemented to combat these imperfections in Raman spectra, experimental methods such as shifted excitation and computational methods such as morphological filtering (Mª José Tosina Muñoz, n.d.) and polynomial algorithms are used to suppress noise from high and low frequency highlighting the advantage of seconds in terms of low cost and ease of implementation, however, the implementation of these methods involves computation time especially when we preprocess large amounts of Raman signals, for this reason we decided to use Parallel computing with multicore technology to optimize the response time of the preprocessing of large volumes of Raman spectroscopic signals in samples of minerals.

In Table 1 we can observe the sequential and parallel processing time what takes for the suppression of fluorescence and shot noise in Raman spectra of minerals. On this occasion we use our entire database to consult the processing time in large volumes of data. It was used the moving averages filtering to smooth the signal as a previous step to operations of the developed ANFIS algorithm, which provides a close baseline in the regions where there are Raman bands which are subtracted from the raw Raman spectrum leaving the signal in the base band. To eliminate the shot noise on signal f, we use a moving average filter with a window size of N = 7, guaranteeing smoothing of the signal without damaging the identifying characteristics of the spectrum.

The arithmetic mean in this case is calculated as:

$$MA = \frac{\sum_{i=1}^{N}(f)}{N} \quad (7)$$

ECORFAN® All rights reserved

In equation (7), N is the base of moving averages. Although there is no specific rule on how to select the bases for moving averages (N), it is recommended that N be large when the behavior of the data is stable over time. Conversely, if the variable shows changing patterns; it is recommended to use a small value of N. In practice, values for N between 2 and 10 are normal.

Raman Spectra	ANFIS Algorithm and Moving Averages Filter	
Mining Examples	Sequential Process (Seg)	Parallel Process (Seg)
10	4.064	3.611
100	41.708	18.644
300	122.304	49.286
500	198.434	79.698
700	276.138	110.399
900	353.525	142.045
1100	428.817	178.942
1300	526.259	222.955
2600	996.946	425.122
5200	2016.7	911.549
10400	4106.3	1817.77

Table 1 Sequential and parallel processing times in suppression of fluorescence and shot noise in Raman spectra of minerals

As we can see in **¡Error! No se encuentra el origen de la referencia.**, we started with 10 spectra of samples of mineral, we continued with increments until we achieve the suppression of fluorescence and shot noise of 10400 Raman spectra of different minerals.

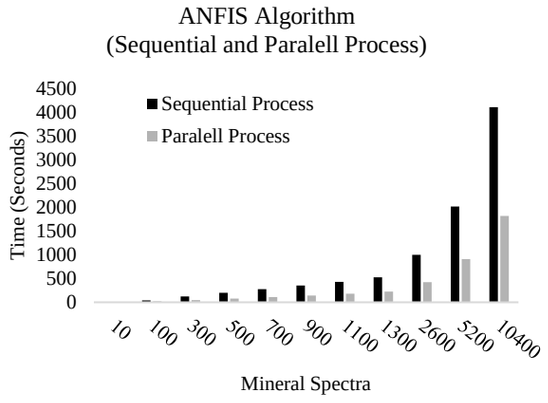

Figure 13 Sequential and Parallel Processing Time using the ANFIS algorithm to eliminate the fluorescence background and moving averages filtering for high frequency noise (shot noise)

In the graph in ***¡Error! No se encuentra el origen de la referencia.***, we clearly observe that we obtain an improvement in the processing time of the data for the elimination of fluorescence and high frequency noise when we implement the ANFIS algorithm and the filtering of moving averages with multicore technology to the set of mineral spectra (data parallelism), we can clearly observe the significant reduction in processing time with a gain of approximately 53.60%.

5. Acknowledgments

The authors thank the collaborators of the RRUFF Project for sharing their database with the scientific community for the benefit of science.

6. Conclusions

A Raman spectrum is a fingerprint of the material being analyzed since it is composed of (a) Raman scattering (RS), which characterizes the molecular composition of the sample through the position of the Raman peaks described by the wave number; there are also numerous disturbances that are added to the spectrum during the measurement process such as: (b) fluorescence noise, and (c) shot noise, sometimes these are several orders of magnitude greater than the useful signal so that could be masked making it difficult to appreciate correctly, for this reason it must be eliminated.

We used an own algorithm based on ANFIS (Adaptive Neuro Fuzzy Inference System) to reveal the fluorescence background of the spectra and the filtering of moving averages to eliminate the shooting noise; both disturbances, causing the masking of the data and the difficult appreciation of its useful content. This preprocessing takes considerable computation time when we process large amounts of Raman spectroscopic signals.

In this work we have shown that it is possible to optimize the preprocessing time of large volumes of Raman spectroscopic signals in samples of minerals through parallel processing that consists of dividing the tasks to be performed in a multicore environment. This optimized method can have specific applications in the field of medicine or industry since it guarantees to carry out diagnostic and classification applications in a considerably small time.

ISSN 2524-2121
ECORFAN® All rights reserved

References

Cartagena, U. P. D. E., Juan, A., Rodríguez, F., & Autor, E. (2010). *Programación Matlab En Paralelo Sobre Clúster Computacional : Evaluación De Prestaciones*.

Crippa, M., Legnaioli, S., Kimbriel, C., & Ricciardi, P. (2020). New evidence for the intentional use of calomel as a white pigment. *Journal of Raman Spectroscopy*, (March), 1–8. https://doi.org/10.1002/jrs.5876

De Faria, D. L. A., Venâncio Silva, S., & De Oliveira, M. T. (1997). Raman microspectroscopy of some iron oxides and oxyhydroxides. *Journal of Raman Spectroscopy*, *28*(11), 873–878. https://doi.org/10.1002/(sici)1097-4555(199711)28:11<873::aid-jrs177>3.0.co;2-b

Gao, W., Kemao, Q., Wang, H., Lin, F., & Seah, H. S. (2009). Parallel computing for fringe pattern processing: A multicore CPU approach in MATLAB® environment. *Optics and Lasers in Engineering*, *47*(11), 1286–1292. https://doi.org/10.1016/j.optlaseng.2009.04.018

Gebrekidan, M. T., Knipfer, C., & Braeuer, A. S. (2020). Vector casting for noise reduction. *Journal of Raman Spectroscopy*. https://doi.org/10.1002/jrs.5835

Gebrekidan, M. T., Knipfer, C., Stelzle, F., Popp, J., Will, S., & Braeuer, A. (2016). A shifted-excitation Raman difference spectroscopy (SERDS) evaluation strategy for the efficient isolation of Raman spectra from extreme fluorescence interference. *Journal of Raman Spectroscopy*. https://doi.org/10.1002/jrs.4775

Gillet, P., Biellmann, C., Reynard, B., & McMillan, P. (1993). Raman spectroscopic studies of carbonates part I: High-pressure and high-temperature behaviour of calcite, magnesite, dolomite and aragonite. *Physics and Chemistry of Minerals*, *20*(1), 1–18. https://doi.org/10.1007/BF00202245

Ishikawa, S. T., & Gulick, V. C. (2013). An automated mineral classifier using Raman spectra. *Computers and Geosciences*, *54*, 259–268. https://doi.org/10.1016/j.cageo.2013.01.011

Jang, J.-S. R., Sun, C.-T., & Mizutani, E. (1997). Neuro-Fuzzy and Soft Computing: A Computational Approach to Learning and Machine Intelligence. In *Prentice Hall*.

Javier, F., Rosas, L., Cesar, J., Romo, M., Veloz, G. M., Contreras, J. R. M., … México, A. (2018). *Optimal Design in the Removal of Fluorescence and Shot Noise in Raman Spectra from Biological Samples*. 78–84.

Lieber, C. A., & Ahadevan-jansen, A. M. (2003). *Automated Method for Subtraction of Fluorescence from Biological Raman Spectra*. *57*(11), 1363–1367.

Mª José Tosina Muñoz, R. P. P. (n.d.). *Filtro Morfológico, eliminacion de fluorescencia*.

Martens, W. N., Rintoul, L., Kloprogge, J. T., & Frost, R. L. (2004). Single crystal raman spectroscopy of cerussite. *American Mineralogist*, *89*(2–3), 352–358. https://doi.org/10.2138/am-2004-2-314

Prajapati, V. (2013). *Big Data Analytics with R and Hadoop*. Retrieved from http://books.google.com/books?hl=en&lr=&id=8eotAgAAQBAJ&oi=fnd&pg=PT12&dq=Big+Data+Analytics+with+R+and+Hadoop&ots=vdKhha6hNe&sig=umigf1-1Rbqs-d-Bp5itHKxNEJA

Soberón-celedón, C. C., Molina-contreras, J. R., Frausto-reyes, C., & Carlos, J. (2016). *Removal of fluorescence and shot noises in Raman spectra of biological samples using morphological and moving averages filters*. *0869*(3), 14–19.

Sugeno, M., & Kang, G. T. (1988). Structure identification of fuzzy model. *Fuzzy Sets and Systems*, *28*(1), 15–33. https://doi.org/10.1016/0165-0114(88)90113-3

Takagi, T., & Sugeno, M. (1984). Derivation of Fuzzy Control Rules From Human Operator'S Control Actions. *IFAC Proceedings Series*, *16*(13), 55–60. https://doi.org/10.1016/S1474-6670(17)62005-6

ISSN 2524-2121
ECORFAN® All rights reserved

Übeyli, E. D. (2008). Adaptive neuro-fuzzy inference system employing wavelet coefficients for detection of ophthalmic arterial disorders. *Expert Systems with Applications*, *34*(3), 2201–2209. https://doi.org/10.1016/j.eswa.2007.02.020

Yeh, Y. T., Gulino, K., Zhang, Y. H., Sabestien, A., Chou, T. W., Zhou, B., … Terrones, M. (2020). A rapid and label-free platform for virus capture and identification from clinical samples. *Proceedings of the National Academy of Sciences of the United States of America*, *117*(2), 895–901. https://doi.org/10.1073/pnas.1910113117

Zhao, J., Lui, H., Mclean, D. I., & Zeng, H. (2007). Automated autofluorescence background subtraction algorithm for biomedical raman spectroscopy. *Applied Spectroscopy*, *61*(11), 1225–1232. https://doi.org/10.1366/000370207782597003

ISSN 2524-2121
ECORFAN® All rights reserved

Article **ECORFAN Journal- Taiwan**
December, 2020 Vol.4 No.8 13-19

Artificial vision system for the prevention of injuries in the upper back and neck areas based on the OpenPose algorithm

Sistema de visión artificial para la prevención de lesiones en las zonas de espalda alta y cuello basado en el algoritmo de OpenPose

GARCÍA-CERVANTES, Heraclio†*, CARDONA-VILLALPANDO, Juan Carlos, BLANCO-MIRANDA, Alan David and CARRILLO-HERNÁNDEZ, Didia

Universidad Tecnológica de León

ID 1st Author: *Heraclio, García-Cervantes* / **ORC ID**: 0000-0002-4229-9229, **Researcher ID Thomson**: X-5622-2019, **CVU CONACYT ID**: 290829

ID 1st Coauthor: *Juan Carlos, Cardona-Villalpando* / **ORC ID**: 0000-0002-2571-892X, **Researcher ID Thomson**: ABF-1633-2020, **CVU CONACYT ID**: 1095804

ID 2nd Coauthor: *Alan David, Blanco-Miranda* / **ORC ID**: 0000-0002-8595-8634, **Researcher ID Thomson**: W-9701-2019, **CVU CONACYT ID**: 298274

ID 3rd Coauthor: *Didia, Carrillo-Hernández* / **ORC ID**: 0000-0001-9989-5884, **Researcher ID Thomson**: ABF-4839-2020, **CVU CONACYT ID**: 936937

DOI: 10.35429/EJT.2020.8.4.13.19 Received October 12, 2020; Accepted December 06, 2020

Abstract

Computer vision is a tool used to understand images that have been analyzed and processed. And in health and human body applications it is no exception, since they help to vectorize the body and its movement, analyzing the changes between them. The main objective of this work is to develop an interactive mobile application for the monitoring, description and recording of body postures in the neck and upper back areas when using cellular devices. The OpenPose algorithm is used to identify and register the specific points of the established zones. In the analysis process, the Keras framework is used in order to build a deep learning convolutional neural network. A graphical user interface is designed in order to facilitate the use and interpretation of measurements. In addition, it is accompanied by an alert system sent when the maximum load angle accepted by the neck in an adult is exceeded (30 ° with respect to the imaginary vertical line on the back). This work contributes to the prevention of future injuries in the cervical areas according to the information provided by specialists in physical rehabilitation.

Artificial Vision, OpenPose, Text Neck

Resumen

La visión artificial es una herramienta usada para comprender imágenes que se han analizado y procesado. Y en aplicaciones de la salud y cuerpo humano no es la excepción, ya que ayudan a vectorizar el cuerpo y su movimiento, analizando los cambios entre los mismos. El objetivo principal del presente trabajo es el de desarrollar una aplicación móvil interactiva para el monitoreo, descripción y registro de las posturas corporales en las zonas del cuello y la espalda alta al hacer uso de dispositivos celulares. Se hace uso del algoritmo de OpenPose para identificación y registro de los puntos específicos de las zonas establecidas. En el proceso de análisis, el framework de Keras es utilizado con la finalidad de construir una red neuronal convolucional de aprendizaje profundo. Se diseña una interfaz gráfica de usuario con la finalidad de facilitar el uso e interpretación de mediciones. Además, se acompaña de un sistema de alerta enviada al sobrepasar el ángulo de carga máximo aceptado por el cuello en una persona adulta (30° respecto a la línea vertical imaginaria en la espalda). Este trabajo contribuye en la prevención de futuras lesiones en las zonas cervicales de acuerdo con la información proporcionada por especialistas en rehabilitación física.

Visión Artificial, OpenPose, Text Neck

Citation: GARCÍA-CERVANTES, Heraclio, CARDONA-VILLALPANDO, Juan Carlos, BLANCO-MIRANDA, Alan David and CARRILLO-HERNÁNDEZ, Didia. Artificial vision system for the prevention of injuries in the upper back and neck areas based on the OpenPose algorithm. ECORFAN Journal-Taiwan. 2020. 4-8: 13-19

* Correspondence to Author (email: hgarcia@utleon.edu.mx)
† Researcher contributing as first author.

© ECORFAN Journal-Taiwan

Introduction

Text Neck

All technological advances have consequences and smart devices are no exception. Today's life of people centers on a mastery of computer technology. The excessive use of the mobile device in daily life tasks induces a problem called "Text Neck" (TN) [I, II], which affects the world population. TN, or "turtleneck posture", is an injury caused by repeated stress and pain from poor position in the use of electronic devices for long periods of time. Symptoms include pain in the neck, shoulders, head, and a change in the curvature of the spine [I – V]. If this syndrome is not treated or is corrected at the right time, the damage can be permanent, causing inflammation of the neck ligaments, muscles, tendons and nerves, which can lead to permanent arthritic changes [IX]. It can also cause a flattening of the spinal curve, early arthritis, compression of the disc, herniated disc etc. It is a health problem that is increasing and affects a large number of the population around the world.

The vertebral column is a bony network that protects the spinal cord, it is inserted at the base of the brain, at the level of the neck and ends at the hip; see figure 1. The upper area, trunk and neck is the part where the injury and musculoskeletal problems occur due to poor posture when using the mobile phone [VI].

Figure 1 Pain area [6]

Users by adopting a prolonged posture when tilting their head towards the screen of the mobile device directly affects the spine, considering that depending on the degrees of inclination of the head, their weight increases depending on the angle, see Figure 2.

There Reports where studies have been made on the time that people spend on average using the mobile, it is concluded that it is a range that goes from 2.7 to 5.4 hours on average a person uses their device daily. The TN epidemic has become a global problem, it is identified that people who present pain in the neck and shoulders tend to have a higher level of anxiety and / or depression due to frequent discomfort. [VII].

Mobile devices are updated frequently, every day there are more applications so that people not only send messages or calls, but also contain games, books, music, cameras, videos, bank account, purchases, whatsapp, facebook, GPS , etc. By replacing a large number of activities allowing them to be carried out in a single device and the movement of people is restricted [I]. Given the circumstances, the Chiropractic and Physiotherapy Associations recommend limiting the activities of mobile devices, using computer equipment to answer emails or call instead of sending messages to avoid NT [VIII].

In a correct posture to avoid TN syndrome, the ears are aligned with the shoulders and shoulder blades, reducing the stress on the spine, see figure 2 first image [V, VI]. According to the angle of inclination of the head, the force exerted on the cervical increases considerably, which is the main cause of the discomfort and problems caused by poor posture, as shown in Figure 2.

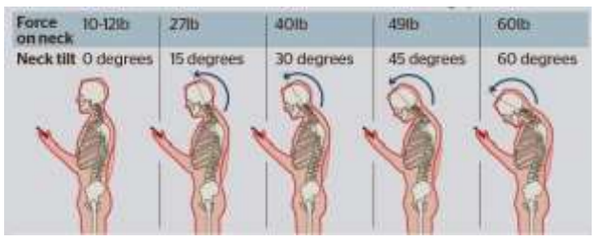

Figure 2 Variation of the force exerted by the head on the spinal column as the degree of inclination increases [VI]

One of the most important aspects for human beings is health, and we must constantly innovate in the development of new tools that allow us to analyze the different diseases that appear every day. Technological development always brings consequences and in this case it is no exception.

ISSN 2524-2121
ECORFAN® All rights reserved

The advancement in electronic devices, with a greater number of applications, causes people to spend more time using the mobile device, which causes stress on the upper part of the spine, which can be aggravated in injuries. TN syndrome is a relatively new health problem, but it is constantly growing due to the constant and excessive use of the mobile device, and development should begin for an efficient study in detecting it early and avoiding complication. This problem is found specifically in the area of the head, neck and back, since it is the part that we force when tilting the head to observe the cell phone. This inclination is the one that needs to be measured by means of its angle that determines the presence or absence of the syndrome and with it the detection of the body's posture, see figure 3.

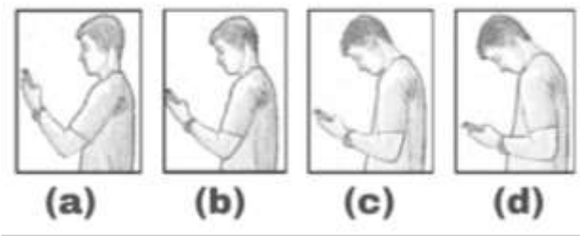

Figure 3 Different positions for viewing the mobile device [X]

TN syndrome is a problem in which it is necessary to intervene immediately, since around 67% of the world population uses cell phones. To carry out a correct approach it is necessary to be clear about the physiological effects that the use of technologies can cause. For this particular case, we will address the problem that cell phone use brings with it, and propose a solution to reduce or eradicate the negative effects caused by the use of smart devices.

The investigation of the technology of recognition of the posture in the use of the mobile, belongs to a branch of the investigation of the estimation of the posture of the human body. Before 2015, the coordinates of the joints were returned directly [XIII], then the literature [XIV] proposed the CPM method that uses a sequential convolutional architecture to express spatial information and texture information. The literature [XV] proposed an hourglass-type network structure, and most of the estimation algorithms for single-person Pose that appeared after 2016 are based on this model structure [XVI, XVII]

In this article, the OpenPose algorithm [XVIII, XIX] is used to extract the characteristics of the spatial positions of the central point of the neck and nose, and how this line is inclined with respect to an imaginary vertical line of the center of the upper back . The extracted feature maps marked with the bony nodes of the volunteers are used as a training set. Then, the Keras deep learning framework is used to build a deep learning network and thus the data set is used for network training. So that the model can be used to judge the posture during the use of a person's mobile in real time and generate alerts when the neck tilt limit is exceeded, thus avoiding excessive loads in the established area.

Methodology

Neural Networks

The brain is made up of nerve cells which connect with each other to form neural networks, where information received from the environment is received and processed. To later be sent to all systems of the body and perform the action.

A neural network is a processor of information which can be stored and available when needed.

There are different learning techniques that can be used in a variety of applications, among them, convolutional neural networks (CNN), which have attracted attention in recent years in vision systems and image analysis [48-50, medical image]. CNNs recognize visual patterns directly from raw image pixels. These networks look at small moles of the input image through neurons of several layers and different weights in each convolution, see Figure 4.

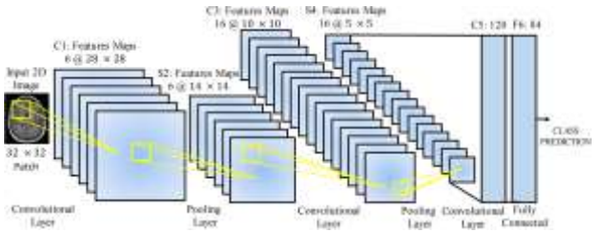

Figure 4 Architecture of a convolutional neural network for image classification. [XI]

ECORFAN® All rights reserved

Each neuron or node in a CNN is governed by an activation function, which controls the output. Activation functions can be linear, sigmoid, tanh, rectified linear unit. In addition to using different types of grouping to split the image, reduce calculations, replace blocks, activate regions, etc. [XII].

In this research, convolutional neural networks will be used, these are the most frequently used for computer vision and are built of a series of layers that process the input image through filters in each convolution, which are the basis of the OpenPose algorithm.

OpenPose algorithm

One tool for extracting human posture is OpenPose. The OpenPose Human Body Attitude Recognition Project is an open source library developed by Carnegie Mellon University (CMU) based on convolutional neural networks and supervised learning and developed in the caffe framework [XVIII]. An estimate of attitude, such as human movement, facial expression, and proper finger movement can be achieved for one or more people, with excellent robustness [XIX]. OpenPose provides a bottom-up approach to real-time estimation of multi-person gestures without the need for character detectors.

When loading the pre-trained OpenPose model, the algorithm will extract 18 body joints and 17 connection lines, see Figures 5 and 6. In the case of this work, only the points corresponding to the nose, neck, right shoulder and shoulder will be taken into account. left.

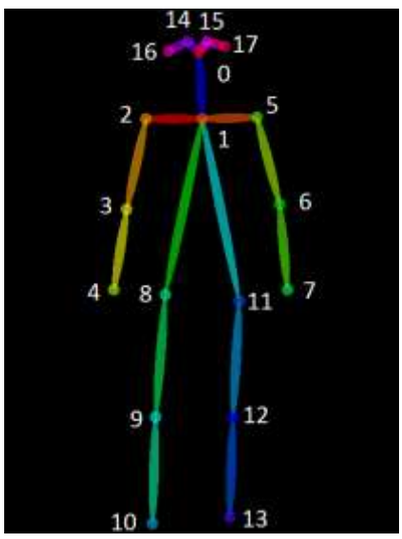

Figure 5 Skeleton data delivered by the OpenPose algorithm

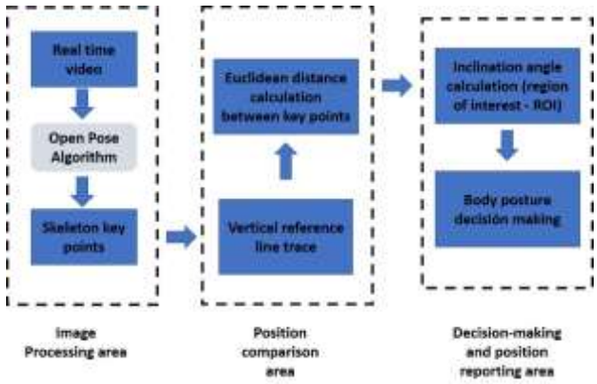

Figure 6 System architecture

Results

The results obtained with the implementation of the OpenPose algorithm in detecting the different postures of people while using the cell phone are shown below.

The generated interface shows the real-time visualization of the person's posture together with the key points, in addition to the lines that join them to show the posture (see Figure 8), while in Figure 7 a list appears with the coordinates of these points.

```
Time Taken in forward pass = 1.446131706237793
Keypoints - Nariz : [(264, 40, 0.7905143)]
Keypoints - Cuello : [(243, 70, 0.5294146)]
Keypoints - D-Hmbr : [(242, 75, 0.6484553)]
Keypoints - D-Codo : [(243, 121, 0.778859)]
Keypoints - D-Mñc : [(257, 164, 0.75650746)]
Keypoints - I-Hbr : [(245, 69, 0.42906943)]
Keypoints - I-Codo : []
Keypoints - I-Mñc : []
Keypoints - D-Cdr : [(243, 163, 0.4876796)]
Keypoints - D-Rod : [(242, 229, 0.507993)]
Keypoints - D-Tob : [(236, 294, 0.70241106)]
Keypoints - I-Cdr : [(258, 157, 0.28631285)]
Keypoints - I-Rod : [(244, 229, 0.11364006)]
Keypoints - I-Tob : [(243, 287, 0.14518315)]
Keypoints - D-Ojo : [(258, 33, 0.7793208)]
Keypoints - I-Ojo : []
Keypoints - D-Orj : [(243, 39, 0.8878803)]
Keypoints - I-Orj : []
```

Figure 7 Coordinates of key points recorded by the OpenPose algorithm

Among the tests carried out, a webcam (VGA resolution) is used, capturing from the front and from the side.

In Figure 8, an example of registration is shown for the points from the shoulders to the head (this being the region of interest for the analysis).

ISSN 2524-2121
ECORFAN® All rights reserved

Figure 8 a) Positions of key points recorded by the OpenPose algorithm, b) Junction lines between key points for tilt angle measurement

Within the developed interface, when starting the video, the image with the line and the angle of inclination in the posture of the person are shown in Figure 9. Here the individual is within the range of the angle of inclination of the head of a proper position, because it shows an angle of 14.35.

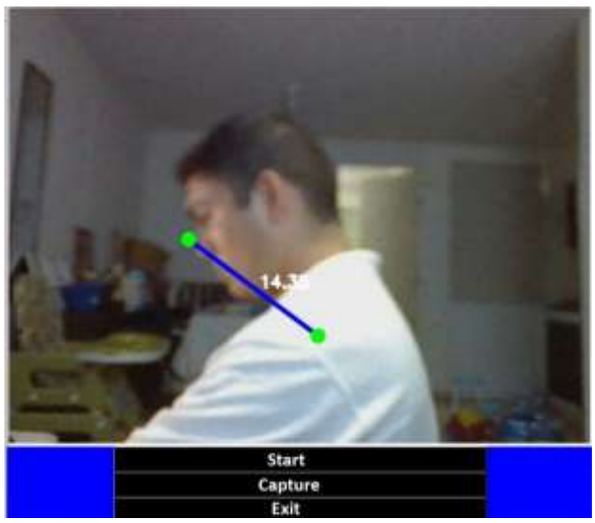

Figure 9 Measurement of head and neck tilt angle during cell phone use

According to what has been reviewed in the literature [VI], the critical angle to generate a posture alert is 15 ° since excessive tension is generated for that angle of inclination and higher, which can cause future injuries. In order to create a warning about this situation, the application sends a push notification [XX] to the person and on the screen changes the color of the line that measures the angle to red, this being a visual alert (Figure 10).

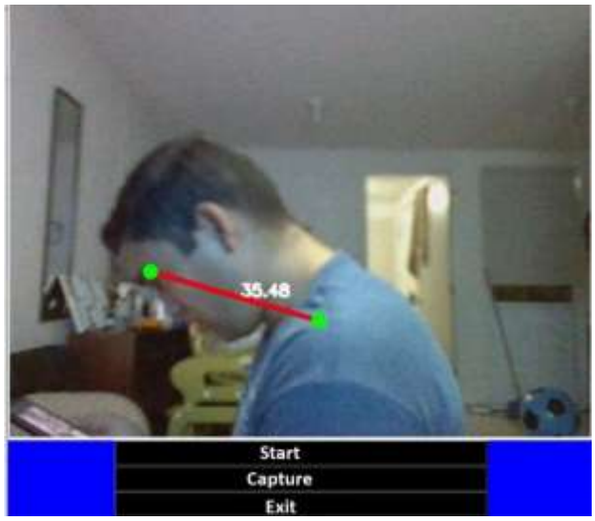

Figure 10 Detection of a high angle of inclination, with a bad posture when using the cell phone

The notification received by the user on his cell phone can be personalized and preset from the system settings. Figure 11 shows an example of the message received during a posture alert.

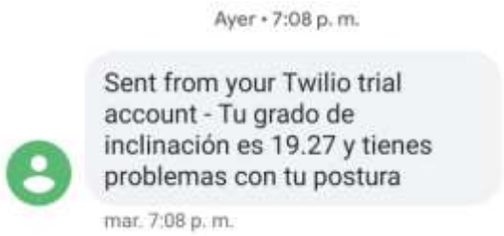

Figure 11 Alert message sent by the developed interface

Acknowledgments

Thanks to the Technological University of León for the space and technical equipment provided to carry out this project. Also, to the physiotherapists Juan Pablo Lira and Armando Correa for the facilities provided for the information and documentation of this work.

Conclusions

In this work, a tilt recognition system was developed in the neck and upper back area, while using mobile devices, based on computer vision to find and correct poor posture in users.

The algorithm uses OpenCV to extract the video information captured by the monitor. Then OpenPose is used to extract the posture feature.

ISSN 2524-2121
ECORFAN® All rights reserved

A pre-trained network model was used, it was used to identify the posture during the use of the mobile device and the sending of notifications to the user when it exceeds the maximum allowed angle.

After actual testing, the user's tilt angle can be effectively identified, helping to develop good habits and prevent future injury to the tested area. It is very significant to reinforce learning in an area that is currently growing more and more and that takes great value from what is expected of new technologies, in favor of human health.

As a future development, the system will be implemented in a convolutional neural network using the Keras deep learning framework to train data sets taken from a physical rehabilitation room, where experts in the area will validate the delivered results and a statistical analysis will be generated. of its precision.

This study also opens up the possibility of attending to other types of alterations or disorders of the upper back and neck, such as cervical rectifications, the result of automobile or sports accidents.

References

[I] Vate U-Lan, P. (2015). "Text Neck Epidemic: a Growing Problem for Smart Phone Users in Thailand". Vol 23, No 3, pp27-32.

[II] Gupta, V.K., Arora, S., and Gupta, M. (2013). "Computer-related illnesses and Facebook syndrome: what are they and how do we tackle them". Med Update, Vol. 23, pp. 676-9.

[III] Park, J., Kim, J., Kim, K., Kim, N., Choi, I., Lee, S., and Yim, J. (2015). "The effects of heavy smartphone use on the cervical angle, pain threshold of neck muscles and depression".

[IV] Park, J., Kim, K., Kim, N., Choi, I., Lee, S., Tak, S., and Yim, J. (2015). "A Comparison of Cervical Flexion, Pain, and Clinical Depression in Frequency of Smartphone Use". Int. J. Bio-Sci. Bio- Technol., Vol. 7, No. 3, pp. 183-190.

[V] Hansraj, K.K. (2014). "Assessment of stresses in the cervical spine caused by posture and position of the head". Surg. Technol. Int.

[VI] Neupane, S, Ifthikar, U.T. and Mathew, A. (2017). "Text Neck Syndrome - Systematic Review", vol-23, No 3, pp 141-148.

[VII] Isaac, C. "Potential Negative Effects Toward Health and Well-Being in Relation to Smart Device Use". the Highlands College at Digital Commons @ Montana Tech, 2014.

[VIII] The American Chiropractic Association (ACA). "Preventing Text Neck". Preventing Text Neck, Oct-2011. <http://www.acatoday.org/JacaDisplay1. cfm?CID= 4637&DisType=PDF>. Accessed 20 October 2015.

[IX] Samani, P.P., Athavale, N.A., Shyam, A. and Sancheti, A.K. (2018). Awareness of text neck syndrome in young-adult population, vol-5, No 8, pp 3335.

[X] Moreira-Damasceno, G., Sá-Ferreira, A. Calazans-Nogueira, L. A., Jandre-Reis, F. J., Santana-Andrade, I. C. and Meziat-Filho, N. (2018). Text neck and neck pain in 18–21-year-old young adults, European Spine Journal, vol-27, pp-1249–1254.

[XI] Anwar, S.M., Majid, M., Qayyum, A., Awais, M., Alnowami, M. and Khan, M. K. (2018). Medical Image Analysis using Convolutional Neural Networks: A Review, J Med Syst, vol-42, pp-226.

[XII] LeCun, Y., Bengio, Y., and Hinton, G.,(2015). Deep learning. Nature. vol-521,pp-436-444.

[XIII] Toshev A, Szegedy C. DeepPose: Human Pose Estimation via Deep Neural Networks [J]. 2013.

[XIV] Wei S E, Ramakrishna V, Kanade T, et al. Convolutional Pose Machines [C]// CVPR. IEEE, 2016.

[XV] Newell A, Yang K, Deng J. Stacked Hourglass Networks for Human Pose Estimation [J]. 2016.

[XVI] Yang W, Li S, Ouyang W, et al. Learning Feature Pyramids for Human Pose Estimation [J]. 2017.

ISSN 2524-2121
ECORFAN® All rights reserved

[XVII] Ke L, Chang M C, Qi H, et al. Multi-Scale Structure-Aware Network for Human Pose Estimation [J]. 2018.

[XVIII] Cao Z, Simon T, Wei S E, et al. Realtime Multi-Person 2D Pose Estimation using Part Affinity Fields [J]. 2016.

[XIX] Qiao S, Wang Y, Jian L. Real-time human gesture grading based on OpenPose [C]// 2017 10th
International Congress on Image and Signal Processing, BioMedical Engineering and Informatics (CISP-BMEI). 2018.

[XX] Okoshi, Tadashi and Tsubouchi, Kota and Tokuda, Hideyuki, "Real-World Product Deployment of Adaptive Push Notification Scheduling on Smartphones", Association for Computing Machinery, New York, NY, USA. (2019) doi.org/10.1145/3292500.3330732.

ISSN 2524-2121
ECORFAN® All rights reserved

Article **ECORFAN Journal- Taiwan**
December, 2020 Vol.4 No.8 20-23

Characterization of a copper susceptor sensitive to solar IR and UV radiation

Caracterización de un susceptor de cobre sensible a radiación solar IR y UV

ZARATE-CORONA, José*†, TELOXA-REYES, Julio and AGUILAR-GALVAN, Daniel

ID 1st Author: *José, Zarate-Corona*

ID 1st Coauthor: *Julio, Teloxa-Reyes*

ID 2nd Coauthor: *Daniel, Aguilar-Galvan*

DOI: 10.35429/EJT.2020.8.4.20.23 Received October 22, 2020; Accepted December 11, 2020

Abstract

Renewable energies use has become the best alternative to reduce the damage effects due to global warming. In this work it is presented the characterization for a copper susceptor being sensible to IR and UV sun radiation, the susceptor was installed in the focus of a parabolic antenna reaching temperatures around 300°C. The susceptor is elaborated from type "K" thermocouples as transducers from heat energy to electric energy, thermocouples were mounted on a copper bar which received a chemical treatment in order to obtain an oxide film sensible to IR and UV sun radiation it is shown the absorption specters of the film taking as a reference the air absorption spectres measured with a BRUKER® equipment. Thermocouple array consist of 800 elements connected on parallel and series, final setup will be disposed in a configuration able to reduce atmospheric perturbations and absorb the high sun radiation values available at UPTlax Campus, it has been evaluated the effectiveness of the presented technology as a viable proposal that could be an alternative to the conventional silice photovoltaic cells.

Renewable energies, Solar Energy, Susceptor, Thermocouple, Sun Radiation

Resumen

El uso de energías renovables se ha convertido en la mejor alternativa para disminuir los graves efectos del calentamiento global. En el presente artículo se muestra la caracterización de un susceptor de cobre sensible a radiación solar IR y UV el cual fue instalado en el foco de una antena parabólica alcanzando temperaturas alrededor de 300 °C, el susceptor está elaborado a partir de termopares tipo "K" como transductores de energía calorifica a energía eléctrica colocados en una placa de cobre, en la cual se depositó una película de óxido sensible a radiación solar IR y UV, se muestran los espectros de absorción del recubrimiento del cobre tomando como referencia los espectros de absorción del aire, obtenidos con un equipo BRUKER®. El arreglo de termopares consta de 800 elementos conectados en serie y paralelo, el dispositivo final será colocado en una configuración que permita minimizar las perturbaciones atmosféricas aprovechando los altos valores de radiación solar que se tienen en el Campus UPTlax, se ha evaluado la efectividad de la tecnología dando como resultado una propuesta viable que permitirá ser una alternativa a las celdas fotovoltaicas de silicio convencionales

Energías Renovables, Energía Solar, Susceptor, Termopar, Radiación Solar

Citation: ZARATE-CORONA, José, TELOXA-REYES, Julio and AGUILAR-GALVAN, Daniel. Characterization of a copper susceptor sensitive to solar IR and UV radiation. ECORFAN Journal-Taiwan. 2020. 4-8: 20-23

* Correspondence to Author (email: oscar.zarate@uptlax.edu.mx)
† Researcher contributing as first author.

© ECORFAN Journal-Taiwan

Introduction

The traditional way to give the solar radiation susceptors the black color is by placing epoxy paints, which are relatively thick layers reducing the efficiency of capturing solar radiation, in addition they do not withstand high temperatures, in this case, the suceptor will be placed in the focus of a parabolic antenna [1], which gives temperatures around 300 ° C. The coloring of the suceptor proposed in this work is through a chemical deposit creating a thin film of matt black copper oxide.

The coloration of the metals is generated on the surface of the metal, suitably grown to produce a deposit adherent to the metal of colored substances arranged in a very thin layer so as to produce the impression of a uniform coloration that does not influence the metallic character, for which will grow a surface film of copper oxide chemically sensitive to IR and UV radiation. The manufacture of this type of heat energy to electrical energy transducers is important because of the manufacturing technique which is not economically and technologically comparable to the silicon solar cell manufacturing technique.

As a thin coating was used, it turns out that minor variations in the chemical and physical constitution of the metal surface, such as small impurities bound in the manufacture of the alloys, exert a lot of influence on the metallic coloration aspects. From this it follows that the prescriptions for the coloring of metals are in the state of the art.

In section 2 the description of the method is presented, the optimal reaction with which the best result is obtained according to the absorption spectra shown, in section 3 a table with the most relevant experimental results is shown, in section 4, it is presents a brief discussion and some photographs of the prototype of the suceptor, finally in section 5 a general conclusion of the work presented is shown Text written in Times New Roman No.12, single space.

Method description

Matte black copper coloration

There are several ways and methods of coloring copper [2], [3], [4], in this article the simplest and most economical method is shown which is heating a solution of caustic soda to the boiling point, at which Potassium persulfate is added to it by means of the boiling solution and in continuous intense reciprocating movement, a matte black film is formed on the surface that allows even reducing and staining copper imperfections in figure 1 some results are shown.

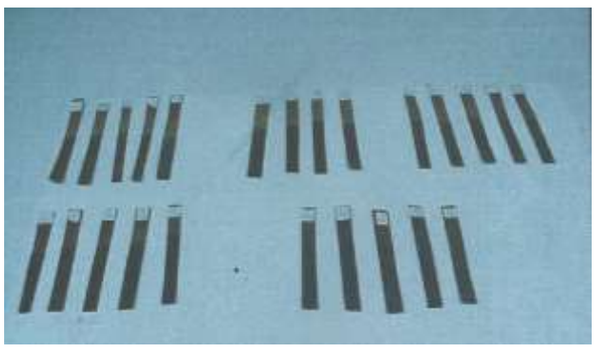

Figure 1 Samples of copper oxide films on copper substrates

Characterization

A characterization of the samples was carried out through the absorption spectra with a Bruker® brand spectrometer. In Figures 2 (a) and 2 (b), IR absorbance spectra are shown for different thickness values of the deposited oxide. In figure 3, the absorption spectrum of air is presented.

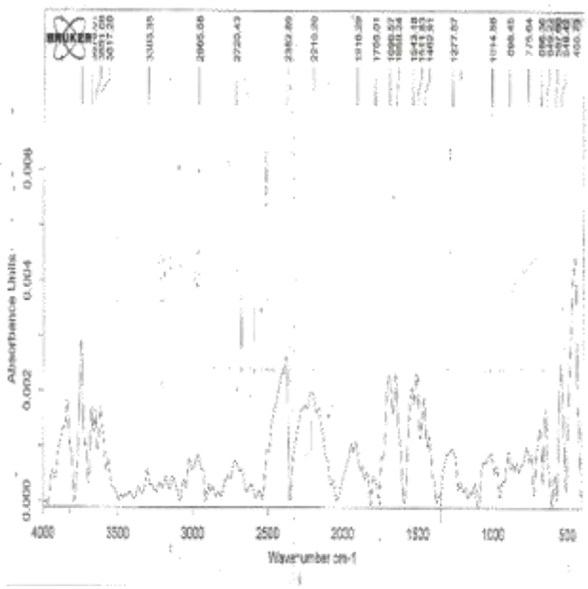

(a)

ECORFAN® All rights reserved

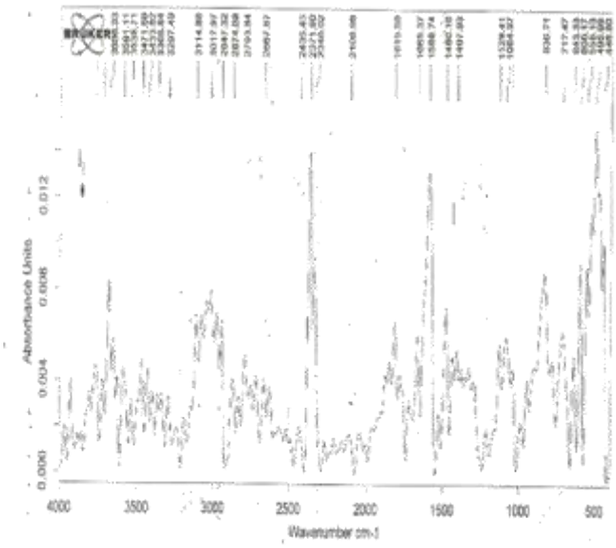

(b)

Figure 2 IR absorbance spectra of samples

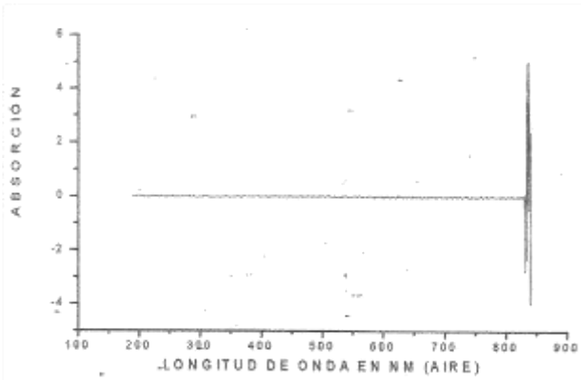

Figure 3 Air absorption spectrum

Figure 4 shows the absorption spectrum with the highest peaks that were obtained, these are corresponding to the wavelength around 597 NM.

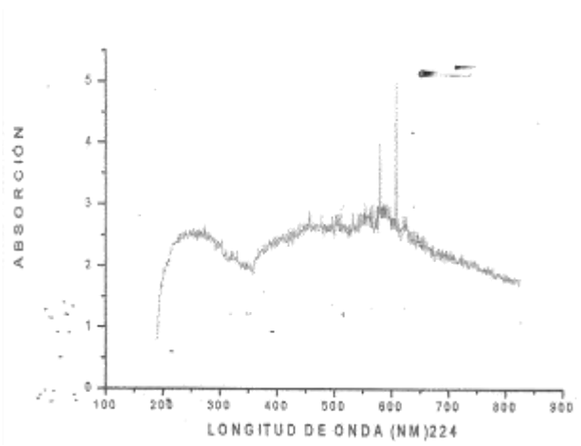

Figure 4 Absorption spectrum with the highest peaks

Figure 5 shows a spectrum with a comparison of the plates with the highest absorption, the maximum absorption at 605 NM wavelength is the upper curve.

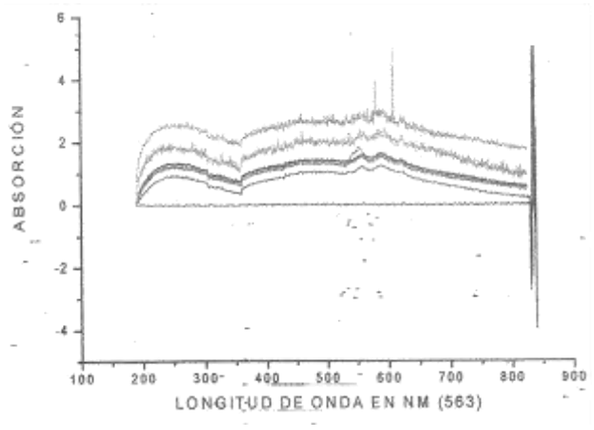

Figure 5 Samples with maximum absorption

Results

Table 1 shows the absorption values for each sample, in which the most relevant values are highlighted.

No. Shows	Average absorbance	No. Shows	Average absorbance
121	1.2	342	1.31
124	1.2	363	1.37
142	1.19	412	1.52
163	1.39	**421**	**1.61**
212	1.33	**424**	**1.58**
221	1.35	442	1.43
224	**3**	463	1.12
242	1.38	**512**	**2.4**
263	1.1	**524**	**1.83**
312	1.31	542	1.45
321	1.33	**563**	**1.54**
324	124	**564**	**1.53**

Table 1 Most relevant values of the samples

Figure 6 shows the increase in the level of absorption between a traditional film and a chemically treated film for IR and UV solar radiation (IR and UV upper curve and with IR sensitive oxide lower curve).

ECORFAN® All rights reserved

Figure 6 Comparison between movies

An experimental measurement was carried out by placing the susceptor in the focus of the parabolic antenna as shown in figure 7.

Figure 7 Satellite dish

Conclusions

Applying the oxidation-reduction technique it was possible to obtain a matte black film with absorbance characteristics in IR and UV, adhesion and durability much better than conventional epoxy paint film.

Thermal efficiency increased by 18% and temperature increased by 21 ºC

With the experimental arrangement it was possible to capture a voltage value of 50mV at a temperature of 230 ° C with a number of 10 thermocouples, it is planned to increase the number of thermocouples in order to use electrical energy to recharge batteries.

Acknowledgments

To the Chemical Engineering laboratory and the Intelligent Computing and Automation Laboratory of the Polytechnic University of Tlaxcala

References

[1]Teloxa Reyes, J & Mendieta Polvo, M. & Zarate Corona, J. & Aguilar Galván, D. (2016) "*Caracterización de Concentrador Solar", Congreso Internacional de Investigación Academia Journals, Tlaxcala, México, Marzo de 2016.*

[2] Introdución a la Térmodinamica en Ingenieria Química Ed. Mc Grall Hill México 1998 Paginas 133-140,730

[3] Enciclopedia Tecnológica de química tomo 15 Nueva Yotk EE.UU., 1997, pagina 676, 677.

[4] Manual del Ingeniero Químico tomo I, Mèxico, 1999, pagina 3-306

ISSN 2524-2121
ECORFAN® All rights reserved

Article **ECORFAN Journal- Taiwan**
December, 2020 Vol.4 No.8 24-27

Comparative study of thermal efficiency of flat spiral vs. conical spiral in a parabolic solar collector

Estudio comparativo de eficiencia térmica de espiral plano vs. espiral cónico en un colector solar parabólico

AVALOS-SANCHEZ, Tomás*†, ROBLES-VELAZQUEZ, Patricia and PRADO-SALAZAR, María

ID 1st Author: *Tomás, Avalos-Sanchez*

ID 1st Coauthor: *Patricia, Robles-Velazquez*

ID 2nd Coauthor: *María, Prado-Salazar*

DOI: 10.35429/EJT.2020.8.4.24.27 Received October 22, 2020; Accepted December 11, 2020

Abstract

Compare the thermal efficiency of two kind of heat by radiant energy concentrated by a parabolic solar collector. Methodology: became two spirals with 1.3 m length and diameter 3/8" copper pipe, which were controlled water flow from one step and recirculated making temperature measurements to water in container return and readings taken every 5 minutes. These coils were placed at the focal point of a parabolic solar collector of 77 cm in diameter and concavity of 6.6 cm. both proved to be very efficient in heat absorption and transmission to the water into itself, which showed greater heat loss but was the conical, although it wasn't exposed to air currents and that it had an aluminum housing. Meanwhile the flat spiral showed greater uniformity in the behavior of temperatures despite being exposed to air currents.The maximum temperature reached, at a flow rate of 0.15 l/min, was 97.5 ° C in 30 minutes from the initial temperature. Lower flows did not allow to make a reliable temperature reading since the water was going into its vapor phase

Parabolic concentrator, Renewable energy, Solar energy, Thermal efficiency, Experimentation, Solar heat exchanger

Resumen

Comparar la eficiencia térmica de dos tipos de focos receptores de energía radiante concentrada por un colector solar parabólico. Metodología: se hicieron dos espirales con 1.3 m de tubo de cobre de 3/8 de diámetro, a los cuales les fueron controlados flujo de agua de un solo paso y recirculada haciendo mediciones de temperatura al agua en el recipiente de retorno y tomado lecturas cada 5 minutos.Estos espirales fueron colocados en el punto focal de un colector solar parabólico de 77 cm de Diámetro y concavidad de 6.6 cm. Ambos mostraron ser muy eficientes en la absorción de calor y la transmisión del mismo al agua, sin embargo, el que mostró mayor pérdida de calor fue el cónico, aunque no estaba expuesto a las corrientes de aire ya que tenía una cubierta de aluminio.Mientras tanto el espiral plano mostró mayor uniformidad en el comportamiento de las temperaturas a pesar de estar expuesto a las corrientes de aire. La temperatura máxima alcanzada, a un flujo de 0.15 litros/min, fue de 97.5 °C en 30 minutos a partir de la temperatura inicial. Los flujos más bajos no permitían hacer una lectura confiable de la temperatura ya que el agua pasaba a su fase vapor.

Concentrador parabólico, Energías renovables, Energía Solar, Eficiencia térmica, Experimentación, Intercambiador solar

Citation: AVALOS-SANCHEZ, Tomás, ROBLES-VELAZQUEZ, Patricia and PRADO-SALAZAR, María. Comparative study of thermal efficiency of flat spiral vs. conical spiral in a parabolic solar collector. ECORFAN Journal-Taiwan. 2020. 4-8: 24-27

* Correspondence to Author (e-mail: tavalos@utj.edu.mx)
† Researcher contributing as first author.

© ECORFAN Journal-Taiwan

Introduction

Solar energy is the renewable energy, for at least the next 5 billion years, most abundant in nature in our solar system; therefore, one of the ways in which it can be channeled for its use is addressed, such as parabolic solar collectors. Throughout history, this type of energy has been used for a wide variety of uses and one of them is to integrate it into industrial processes such as the recovery of water from wastewater.

Two spirals designed and elaborated were compared, each one with its own variables, in order to be used as absorbers of solar radiation, with the purpose of verifying the thermal efficiency of each one when subjecting them to water heating tests and with the obtaining treated water for sanitary use

Solar collectors are structures designed to capture the sun's rays with the aim of transforming them into thermal energy in order to raise the temperature of a fluid or converting it to mechanical energy and transforming it into electrical energy by means of a motor.

Historically, the use of solar energy has occurred in an important way, it began with the development of a method used by Archimedes in the year 212 BC. approximately, he used the solar concentrators to burn the Roman ships by using a large concave mirror

Using solar concentrators with efficient systems of absorption and transmission of that energy in the recovery of fluids or water heating for industrial or domestic use at low cost will be a valuable contribution to mitigate the effects of environmental pollution and the high costs of the fossil fuels. Using 1.3 m 3/8 ”copper tube, two spirals were formed, one flat, Fig 1,
Clearly explain the problem to be solved and the central hypothesis.

Development of Sections and Sections of the Article with subsequent numbering

Hypothesis

In the comparison about the thermal efficiency between a flat spiral and a conical spiral, it is conjectured that the conical spiral will capture in a more efficient way the heat incident on the absorber, since the outer rings of the spiral are closer together.

To the parabolic they absorb heat while transmitting it to the liquid by conduction, in this way when the liquid reaches the heat concentration zone its temperature is higher than that of the environment, reducing the time required to heat the water, if at This system we add thermal insulation and a water recirculation system that is obtained at the exit of the spiral, we will have a higher performance conductor.

Methodology

It was divided into stages: Focal length calculation, flow measurement, temperature measurement.

Focal length calculation

A steel parabolic antenna was used which was polished and sent to chrome to have a mirror finish, Fig. 3. This already had a signal receiver insertion point established, however, it had to be calculated to confirm that it was correct. for the purposes of installing the spirals to be tested. Previously, the distance between the spiral and the concentrator was measured, calling it the real distance, which was 54.4cm. The calculation of the adequate distance that should exist between the plate and the absorber (spiral) was carried out with the following equation:

$$f = D^2/(16 * C) \quad (1)$$

Where: f = Focal length.
D = Diameter of the plate.
C = Depth or concavity of the plate.

Carrying out the measurements required for the equation, we obtain:

C= 6.6cm
D= 77cm
$f = (77)^2/\ (16 * 6.6)$
$f = 56.14cm$

The spirals were placed at the calculated focal length and it was there that the test runs were made.

Flow determination

A container with an approximate water volume of 10L was used, in said container the recirculation pump was installed connected to the two hoses, one connected to the system and the other, which is the return one after passing through the system.

ISSN 2524-2121
ECORFAN® All rights reserved

The valves were calibrated and their positions were determined to obtain the flows at which the runs would be made.

Determination of Temperature

The temperature readings were made with a mercury thermometer from -10 to 110 ° C with a sensitivity of 1 ° C. A thermometer was installed in the container and another in the outlet of the water return hose.

Variables:

Flow: 0.2 l / min, 0.15 l / min and 0.1l / min with and without recirculation of water to the same container.

Spirals: 2
Readings: 6, one every 5 minutes
Total runs: 72

The position of the calculated focal point was adjusted, it was placed in the orientation, with respect to the sun, required depending on the spiral and the position to be evaluated.

The water began to flow through the spiral and when it reached the outlet the digital thermometer marked the measurements obtained from the water.

The readings marked at time intervals were taken, timing every 5 min until reaching 30 min. The final temperature reached in the container was taken.

To start a new cycle of measurements, the container was refilled with water at room temperature. Once the data was obtained, the emptying was done and the corresponding tables and graphs were generated.

Results

The temperature measurements at the different flows resulted in the flat copper spiral having a more uniform behavior with respect to the conical one. The downward temperature variations were minimal under the same weather conditions compared to the conical spiral, even when it was protected from the wind with an aluminum barrier. See graphs 1 to 10

In the flat spiral, the maximum temperature reached of the water at the outlet of the return hose was 97.5 at a flow of 0.1 l / min, see Graph 5, this recirculating the water to the same container, which was increasing the temperature of the inlet water gradually. Under the same conditions, it was not possible to measure with the conical spiral. However, with the latter at a flow of 0.2 l / min and without recirculation, a temperature of 54.9 ° C was obtained. See Graph 10. At a flow of 0.15 l / min with the same climatic conditions, the flat spiral was more efficient since it reached a temperature of 72.6 ° C vs. 32.9 ° C. See Graph 8.

Annexes

Figure 1 Spiral Copper tube, Flat

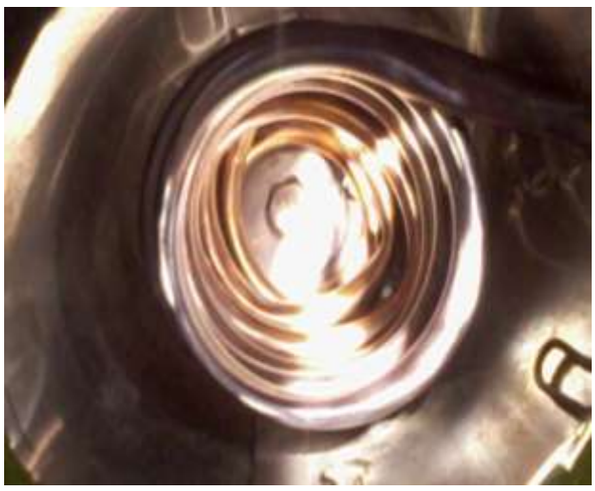

Figure 2 Cone Shaped Copper Tube Spiral

ISSN 2524-2121
ECORFAN® All rights reserved

Figure 3 Mirror Finished Parabolic Concentrator

Acknowledgments

This work was carried out at the facilities of the Technological University of Jalisco, receiving support from it for its realization, for which we extend our gratitude.

Conclusions

The recirculating water condition turned out to be the most recommended to achieve the best temperatures in the water. The parabolic spiral with protection was not the best option, which showed that the hypothesis was negative.

The parabolic solar radiation collector option is subject to too many climatic variables that do not allow it to have a constant behavior all year round, however, it is still a very good option when you want to reach extreme temperatures. Only in this system the thermocouple measurement was made at the focal point and 970 ° C was reached. empirically, a Pyrex glass test tube was placed with water at the focal point and instantly the water began to boil the tube to melt. More tests and new designs of solar radiation collectors are needed.

References

expodime. (s.f.). Recuperado el 2012, de expodime: http://www.expodime.cucei.udg.mx/vexpo/ivexpodime/pdf

luz verde. (s.f.). Recuperado el 2012, de luz verde : http://www.luzverde.org

solar, e. (s.f.). Obtenido de http://energiasolar.911mb.com

mundo solar. (s.f.). Recuperado el 11 de 11 de 2012, de mundo solar: http://www.dforcesolar.com/energia-solar/historia-de-la-energia-solar/

vinculando, r. (2010). energia solar como fuente alterna para el tratamiento de la limpieza de agua. Vinculando

ECORFAN® All rights reserved

[Title in Times New Roman and Bold No. 14 in English and Spanish]

Surname (IN UPPERCASE), Name 1st Author†*, Surname (IN UPPERCASE), Name 1st Coauthor, Surname (IN UPPERCASE), Name 2nd Coauthor and Surname (IN UPPERCASE), Name 3rd Coauthor

Institutional Affiliation of Author including Dependency (No.10 Times New Roman and Italic)

International Identification of Science - Technology and Innovation

ID 1st Author: (ORC ID - Researcher ID Thomson, arXiv Author ID - PubMed Author ID - Open ID) and CVU 1st author: (Scholar-PNPC or SNI-CONACYT) (No.10 Times New Roman)

ID 1st Coauthor: (ORC ID - Researcher ID Thomson, arXiv Author ID - PubMed Author ID - Open ID) and CVU 1st coauthor: (Scholar or SNI) (No.10 Times New Roman)

ID 2nd Coauthor: (ORC ID - Researcher ID Thomson, arXiv Author ID - PubMed Author ID - Open ID) and CVU 2nd coauthor: (Scholar or SNI) (No.10 Times New Roman)

ID 3rd Coauthor: (ORC ID - Researcher ID Thomson, arXiv Author ID - PubMed Author ID - Open ID) and CVU 3rd coauthor: (Scholar or SNI) (No.10 Times New Roman)

(Report Submission Date: Month, Day, and Year); Accepted (Insert date of Acceptance: Use Only ECORFAN)

Abstract (In English, 150-200 words)

Objectives
Methodology
Contribution

Abstract (In Spanish, 150-200 words)

Objectives
Methodology
Contribution

Keywords (In English)

Indicate 3 keywords in Times New Roman and Bold No. 10

Keywords (In Spanish)

Indicate 3 keywords in Times New Roman and Bold No. 10

Citation: Surname (IN UPPERCASE), Name 1st Author, Surname (IN UPPERCASE), Name 1st Coauthor, Surname (IN UPPERCASE), Name 2nd Coauthor and Surname (IN UPPERCASE), Name 3rd Coauthor. Paper Title. ECORFAN Journal-Taiwan. Year 1-1: 1-11 [Times New Roman No.10]

* Correspondence to Author (example@example.org)
† Researcher contributing as first author.

Introduction

Text in Times New Roman No.12, single space.

General explanation of the subject and explain why it is important.

What is your added value with respect to other techniques?

Clearly focus each of its features

Clearly explain the problem to be solved and the central hypothesis.

Explanation of sections Article.

Development of headings and subheadings of the article with subsequent numbers

[Title No.12 in Times New Roman, single spaced and bold]

Products in development No.12 Times New Roman, single spaced.

Including graphs, figures and tables-Editable

In the article content any graphic, table and figure should be editable formats that can change size, type and number of letter, for the purposes of edition, these must be high quality, not pixelated and should be noticeable even reducing image scale.

[Indicating the title at the bottom with No.10 and Times New Roman Bold]

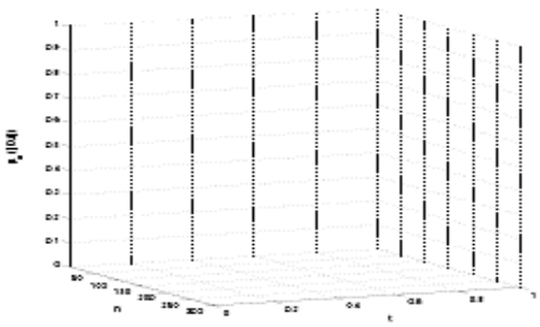

Graphic 1 Title and *Source (in italics)*

Should not be images-everything must be editable.

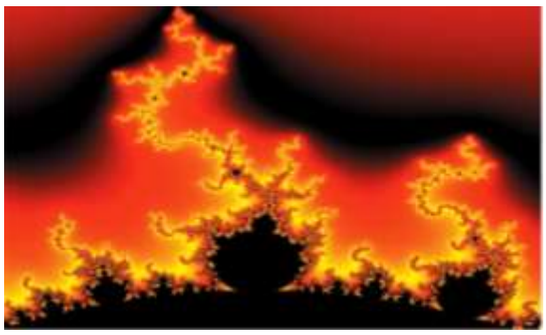

Figure 1 Title and *Source (in italics)*

Should not be images-everything must be editable.

Table 1 Title and *Source (in italics)*

Should not be images-everything must be editable.

Each article shall present separately in **3 folders**: a) Figures, b) Charts and c) Tables in .JPG format, indicating the number and sequential Bold Title.

For the use of equations, noted as follows:

$$Y_{ij} = \alpha + \sum_{h=1}^{r} \beta_h X_{hij} + u_j + e_{ij} \qquad (1)$$

Must be editable and number aligned on the right side.

Methodology

Develop give the meaning of the variables in linear writing and important is the comparison of the used criteria.

Results

The results shall be by section of the article.

Annexes

Tables and adequate sources

Thanks

Indicate if they were financed by any institution, University or company.

Conclusions

Explain clearly the results and possibilities of improvement.

ISSN 2524-2121
ECORFAN® All rights reserved

References

Use APA system. Should not be numbered, nor with bullets, however if necessary numbering will be because reference or mention is made somewhere in the Article.

Use Roman Alphabet, all references you have used must be in the Roman Alphabet, even if you have quoted an Article, book in any of the official languages of the United Nations (English, French, German, Chinese, Russian, Portuguese, Italian, Spanish, Arabic), you must write the reference in Roman script and not in any of the official languages.

Technical Specifications

Each article must submit your dates into a Word document (.docx):

Journal Name
Article title
Abstract
Keywords
Article sections, for example:

1. Introduction
2. Description of the method
3. Analysis from the regression demand curve
4. Results
5. Thanks
6. Conclusions
7. References

Author Name (s)
Email Correspondence to Author
References

Intellectual Property Requirements for editing:

-Authentic Signature in Color of Originality Format Author and Coauthors

-Authentic Signature in Color of the Acceptance Format of Author and Coauthors

ISSN 2524-2121
ECORFAN® All rights reserved

Reservation to Editorial Policy

ECORFAN Journal-Taiwan reserves the right to make editorial changes required to adapt the Articles to the Editorial Policy of the Journal. Once the Article is accepted in its final version, the Journal will send the author the proofs for review. ECORFAN® will only accept the correction of errata and errors or omissions arising from the editing process of the Journal, reserving in full the copyrights and content dissemination. No deletions, substitutions or additions that alter the formation of the Article will be accepted.

Code of Ethics - Good Practices and Declaration of Solution to Editorial Conflicts

Declaration of Originality and unpublished character of the Article, of Authors, on the obtaining of data and interpretation of results, Acknowledgments, Conflict of interests, Assignment of rights and Distribution.

The ECORFAN-Mexico, S.C Management claims to Authors of Articles that its content must be original, unpublished and of Scientific, Technological and Innovation content to be submitted for evaluation.

The Authors signing the Article must be the same that have contributed to its conception, realization and development, as well as obtaining the data, interpreting the results, drafting and reviewing it. The Corresponding Author of the proposed Article will request the form that follows.

Article title:

– The sending of an Article to ECORFAN Journal- Taiwan emanates the commitment of the author not to submit it simultaneously to the consideration of other series publications for it must complement the Format of Originality for its Article, unless it is rejected by the Arbitration Committee, it may be withdrawn.

– None of the data presented in this article has been plagiarized or invented. The original data are clearly distinguished from those already published. And it is known of the test in PLAGSCAN if a level of plagiarism is detected Positive will not proceed to arbitrate.

– References are cited on which the information contained in the Article is based, as well as theories and data from other previously published Articles.

– The authors sign the Format of Authorization for their Article to be disseminated by means that ECORFAN-Mexico, S.C. In its Holding Taiwan considers pertinent for disclosure and diffusion of its Article its Rights of Work.

– Consent has been obtained from those who have contributed unpublished data obtained through verbal or written communication, and such communication and Authorship are adequately identified.

– The Author and Co-Authors who sign this work have participated in its planning, design and execution, as well as in the interpretation of the results. They also critically reviewed the paper, approved its final version and agreed with its publication.

– No signature responsible for the work has been omitted and the criteria of Scientific Authorization are satisfied.

– The results of this Article have been interpreted objectively. Any results contrary to the point of view of those who sign are exposed and discussed in the Article.

Copyright and Access

The publication of this Article supposes the transfer of the copyright to ECORFAN-Mexico, SC in its Holding Taiwan for its ECORFAN Journal- Taiwan, which reserves the right to distribute on the Web the published version of the Article and the making available of the Article in This format supposes for its Authors the fulfilment of what is established in the Law of Science and Technology of the United Mexican States, regarding the obligation to allow access to the results of Scientific Research.

Article Title:

Name and Surnames of the Contact Author and the Coauthors	Signature
1.	
2.	
3.	
4.	

Principles of Ethics and Declaration of Solution to Editorial Conflicts

Editor Responsibilities

The Publisher undertakes to guarantee the confidentiality of the evaluation process, it may not disclose to the Arbitrators the identity of the Authors, nor may it reveal the identity of the Arbitrators at any time.

The Editor assumes the responsibility to properly inform the Author of the stage of the editorial process in which the text is sent, as well as the resolutions of Double-Blind Review.
The Editor should evaluate manuscripts and their intellectual content without distinction of race, gender, sexual orientation, religious beliefs, ethnicity, nationality, or the political philosophy of the Authors.

The Editor and his editing team of ECORFAN® Holdings will not disclose any information about Articles submitted to anyone other than the corresponding Author.

The Editor should make fair and impartial decisions and ensure a fair Double-Blind Review.

Responsibilities of the Editorial Board

The description of the peer review processes is made known by the Editorial Board in order that the Authors know what the evaluation criteria are and will always be willing to justify any controversy in the evaluation process. In case of Plagiarism Detection to the Article the Committee notifies the Authors for Violation to the Right of Scientific, Technological and Innovation Authorization.

Responsibilities of the Arbitration Committee

The Arbitrators undertake to notify about any unethical conduct by the Authors and to indicate all the information that may be reason to reject the publication of the Articles. In addition, they must undertake to keep confidential information related to the Articles they evaluate.

Any manuscript received for your arbitration must be treated as confidential, should not be displayed or discussed with other experts, except with the permission of the Editor.

The Arbitrators must be conducted objectively, any personal criticism of the Author is inappropriate.

The Arbitrators must express their points of view with clarity and with valid arguments that contribute to the Scientific, Technological and Innovation of the Author.

The Arbitrators should not evaluate manuscripts in which they have conflicts of interest and have been notified to the Editor before submitting the Article for Double-Blind Review.

Responsibilities of the Authors

Authors must guarantee that their articles are the product of their original work and that the data has been obtained ethically.

Authors must ensure that they have not been previously published or that they are not considered in another serial publication.

Authors must strictly follow the rules for the publication of Defined Articles by the Editorial Board.

The authors have requested that the text in all its forms be an unethical editorial behavior and is unacceptable, consequently, any manuscript that incurs in plagiarism is eliminated and not considered for publication.

Authors should cite publications that have been influential in the nature of the Article submitted to arbitration.

Information services

Indexation - Bases and Repositories

RESEARCH GATE (Germany)
GOOGLE SCHOLAR (Citation indices-Google)
MENDELEY (Bibliographic References Manager)
HISPANA (Information and Bibliographic Orientation-Spain)

Publishing Services

Citation and Index Identification H
Management of Originality Format and Authorization
Testing Article with PLAGSCAN
Article Evaluation
Certificate of Double-Blind Review
Article Edition
Web layout
Indexing and Repository
ArticleTranslation
Article Publication
Certificate of Article
Service Billing

Editorial Policy and Management

69 Street. YongHe district, ZhongXin. Taipei-Taiwan. Phones: +52 1 55 6159 2296, +52 1 55 1260 0355, +52 1 55 6034 9181; Email: contact@ecorfan.org www.ecorfan.org

ECORFAN®

Chief Editor
VARGAS-DELGADO, Oscar. PhD

Executive Director
RAMOS-ESCAMILLA, María. PhD

Editorial Director
PERALTA-CASTRO, Enrique. MsC

Web Designer
ESCAMILLA-BOUCHAN, Imelda. PhD

Web Diagrammer
LUNA-SOTO, Vladimir. PhD

Editorial Assistant
SORIANO-VELASCO, Jesús. BsC

Translator
DÍAZ-OCAMPO, Javier. BsC

Philologist
RAMOS-ARANCIBIA, Alejandra. BsC

Advertising & Sponsorship

(ECORFAN® Taiwan), sponsorships@ecorfan.org

Site Licences

03-2010-032610094200-01-For printed material ,03-2010-031613323600-01-For Electronic material,03-2010-032610105200-01-For Photographic material,03-2010-032610115700-14-For the facts Compilation,04-2010-031613323600-01-For its Web page,19502-For the Iberoamerican and Caribbean Indexation,20-281 HB9-For its indexation in Latin-American in Social Sciences and Humanities,671-For its indexing in Electronic Scientific Journals Spanish and Latin-America,7045008-For its divulgation and edition in the Ministry of Education and Culture-Spain,25409-For its repository in the Biblioteca Universitaria-Madrid,16258-For its indexing in the Dialnet,20589-For its indexing in the edited Journals in the countries of Iberian-America and the Caribbean, 15048-For the international registration of Congress and Colloquiums. financingprograms@ecorfan.org

Management Offices

69 Street. YongHe district, ZhongXin. Taipei-Taiwan.

ECORFAN Journal-Taiwan

"Optimizing the removal of fluorescence and shot noise in Raman Spectra of minerals by ANFIS and moving averages filter"
CABRERA-CABAÑAS, Reinier, LUNA-ROSAS, Francisco Javier, MARTINEZ-ROMO, Julio César and HERNÁNDEZ-VARGAS, Marco Antonio
Instituto Tecnológico de Aguascalientes

"Artificial vision system for the prevention of injuries in the upper back and neck areas based on the OpenPose algorithm"
GARCÍA-CERVANTES, Heraclio, CARDONA-VILLALPANDO, Juan Carlos, BLANCO-MIRANDA, Alan David and CARRILLO-HERNÁNDEZ, Didia
Universidad Tecnológica de León

"Characterization of a copper susceptor sensitive to solar IR and UV radiation"
ZARATE-CORONA, José, TELOXA-REYES, Julio and AGUILAR-GALVAN, Daniel

"Comparative study of thermal efficiency of flat spiral vs. conical spiral in a parabolic solar collector"
AVALOS-SANCHEZ, Tomás, ROBLES-VELAZQUEZ, Patricia and PRADO-SALAZAR, María

2524 2121
ISSN 2524-2121

www.ecorfan.org